DOI: 10.1534/genetics.107.082966

Functional Characterization of the *dRYBP* Gene in Drosophila

Inma González, Ricardo Aparicio and Ana Busturia[1]

Centro de Biología Molecular CSIC-UAM, Universidad Autónoma de Madrid, Cantoblanco, 28049 Madrid, Spain

Manuscript received October 9, 2007
Accepted for publication May 6, 2008

ABSTRACT

The Drosophila *dRYBP* gene has been described to function as a *Polycomb*-dependent transcriptional repressor. To determine the *in vivo* function of the *dRYBP* gene, we have generated mutations and analyzed the associated phenotypes. Homozygous null mutants die progressively throughout development and present phenotypes variable both in their penetrance and in their expressivity, including disrupted oogenesis, a disorganized pattern of the syncytial nuclear divisions, defects in pattern formation, and decreased wing size. Although *dRYBP* mutations do not show the homeotic-like phenotypes typical of mutations in the PcG and trxG genes, they enhance the phenotypes of mutations of either the *Sex comb extra* gene (PcG) or the *trithorax* gene (*trxG*). Finally, the dRYBP protein interacts physically with the Sex comb extra and the Pleiohomeotic proteins, and the homeotic-like phenotypes produced by the high levels of the dRYBP protein are mediated through its C-terminal domain. Our results indicate that the *dRYBP* gene functions in the control of cell identity together with the PcG/trxG proteins. Furthermore, they also indicate that *dRYBP* participates in the control of cell proliferation and cell differentiation and we propose that its functional requirement may well depend on the robustness of the animal.

PATTERN formation during animal development requires the controlled spatial and temporal regulation of gene expression. Once gene transcriptional states have been established, their maintenance during cellular proliferation is crucial for the normal development of the organism. The *Polycomb* (PcG) and the *trithorax* (trxG) groups of genes play a pivotal role in this process (for a recent review see Schuettengruber *et al.* 2007). The PcG genes are required for the maintenance of the repressed state while the trxG are needed for the maintenance of the active state. The PcG and trxG genes were first identified in the fly *Drosophila melanogaster*, due to their role in morphogenesis as regulators of homeotic gene expression (Lewis 1978; Jürgens 1985; Breen and Harte 1991; for a review see Ringrose and Paro 2004). However, it is now clear that the PcG and trxG genes also have relevant roles in other biological processes, such as hematopoiesis, stem cell renewal, control of cell proliferation, and tumorigenesis (van der Lugt *et al.* 1994; Valk-Lingbeek *et al.* 2004; Brock and Fisher 2005; Ferres-Marco *et al.* 2006; Martinez and Cavalli 2006; Sparmann and Van Lohuizen 2006).

Central to PcG/trxG epigenetic-mediated mechanisms is the recruitment and formation of multimeric protein complexes. In Drosophila, three major protein complexes containing PcG proteins have been isolated. The first identified were the complexes *P*olycomb *r*epressive *c*omplex *1* (PRC1) (Shao *et al.* 1999) and PRC2 (Cao *et al.* 2002; Czermin *et al.* 2002; Kuzmichev *et al.* 2002; Muller *et al.* 2002). The core of PRC1 includes Polycomb (PC), Posterior sex combs (PSC), the E3 ubiquitin ligase Sex comb extra (SCE), and Polyhomeotic (PH). The core of PRC2 is composed of the histone methyl transferase Enhancer of zeste [E(Z)], Suppressor of zeste 12 [SU(Z)12], Extra sex combs (ESC), and Nurf-55. The third repressive complex, *p*leio*ho*meotic *r*epressor *c*omplex (PHORC), containing the pleiohomeotic (PHO) protein, has recently been isolated from Drosophila embryos (Klymenko *et al.* 2006). Three trxG complexes have been identified: *t*rithorax *a*cetylation *c*omplex (TAC), NURF, and the SWI/SNF (for reviews see Grimaud *et al.* 2006b; Schwartz and Pirrotta 2007). There are other PcG/trxG proteins that do not form part of the core of these complexes, but still are associated with them and, therefore, have been classified as PcG/trxG-associated proteins (Otte and Kwaks 2003).

While much is known about the roles of the PcG/trxG proteins in the Drosophila morphogenesis, less is known about their role in biological processes such as the control of cellular proliferation and differentiation during development. Mutations in some of the Drosophila PcG/trxG genes cause phenotypes associated with misregulation of cell proliferation. For example, *E(z)* was identified in a screen for essential cell-cycle genes (Gatti and Baker 1989), and mutations in the *E(z)* gene produce proliferation defects and the appearance of small imaginal discs (Phillips and Shearn 1990). Furthermore, the corto protein (a centrosomal and chromosomal factor) colocalizes with PSC binding

[1]*Corresponding author:* Centro de Biología Molecular Severo Ochoa, Universidad Autónoma de Madrid, Campus de Cantoblanco, c/Nicolás Cabrera 1, 28049 Madrid, Spain. E-mail: abusturia@cbm.uam.es

sites at polytene chromosomes, interacts genetically with PcG mutations, and affects progression through mitosis (Kodjabachian *et al.* 1998). Moreover, mutations in the PcG genes *ph*, *Pc*, and *Psc* show segregation defects during syncytial embryonic mitosis (O'Dor *et al.* 2006). Finally, it has been shown recently that the expression of *cyclin A* is directly regulated by the PcG proteins, showing a clear link between these proteins and the control of the cell cycle (Martinez *et al.* 2006).

To define the mechanisms by which PcG/trxG function, the isolation and functional characterization of each component of the complexes is necessary. The murine *RYBP* gene was identified in a two-hybrid screen designed to isolate Ring1A/Ring1B (SCE in Drosophila) interacting proteins (Garcia *et al.* 1999). Because of its interaction with Ring1A, M33, and YY1 (SCE, PC, and PHO, respectively, in Drosophila)—all of them key components of the PcG complexes—RYBP was proposed to belong to the PcG of proteins (Garcia *et al.* 1999). Studies of the murine RYBP gene and protein indicate that the gene has several distinct biological roles and, because the protein can bind to several transcription factors, it has been proposed to function as an adaptor protein (Garcia *et al.* 1999; Trimarchi *et al.* 2001; Sawa *et al.* 2002; Schlisio *et al.* 2002). It has been shown that the murine RYBP protein is a novel ubiquitin-binding protein that is itself ubiquitinated. Furthermore, one of its targets appears to be the ubiquitinated histone H2A, which is also a substrate of Ring1 B E3 ubiquitin ligase (Arrigoni *et al.* 2006). Recently, a BCOR protein complex has been isolated that, together with the RYBP protein, includes a Posterior sex combs homolog, NSPC1, and RNF2, an E3 ligase with H2A mono-ubiquitylation activity (Gearhart *et al.* 2006; Sanchez *et al.* 2007). Together these results suggest that the interaction of RYBP and RNF2/Ring1A/SCE may be necessary for the mono-ubiquitylation of H2A (Arrigoni *et al.* 2006), an essential mechanism for the maintenance of gene expression (Wang *et al.* 2003; de Napoles *et al.* 2004; Fang *et al.* 2004; Cao *et al.* 2005). Finally, RYBP knockout mice exhibited lethality at the early postimplantation stage, suggesting an essential role in survival. No homeotic phenotypes were reported in these mutants, but the lack of RYBP function in the central nervous system (CNS) produced brain overgrowth and disrupted neural tube closure (Pirity *et al.* 2005).

Previously, we described the identification of the *dRYBP* gene in Drosophila (Bejarano *et al.* 2005). We showed that the dRYBP protein behaves as a *Polycomb*-dependent transcriptional repressor throughout development. Furthermore, we showed that high levels of dRYBP protein produce homeotic-like phenotypes that can be modulated by mutations in PcG/trxG genes. These results suggested that the dRYBP protein could function by recruiting the PcG proteins and, therefore, linked dRYBP to the mechanisms of maintenance of gene expression in Drosophila.

We have studied the biological role of *dRYBP* by characterizing the phenotypes associated with *dRYBP* mutations. The phenotypes associated with *dRYBP* mutations are variable both in their expressivity and in their penetrance. *dRYBP* mutations are pleiotropic, producing progressive lethality during development, arrest in the syncytial nuclear divisions, defects in morphogenesis, reduced size of the wings, and cell differentiation defects. Although *dRYBP* mutations alone do not result in homeotic-like phenotypes, they do when in combination with mutations in some *PcG* and *trxG* genes. We have found that the dRYBP protein is localized in a nuclear pattern and colocalizes with some of the Polycomb nuclear bodies (Buchenau *et al.* 1998; Saurin *et al.* 1998; Netter *et al.* 2001; Ficz *et al.* 2005; Grimaud *et al.* 2006a). Moreover, the protein is dynamically distributed during the mitotic cycle in the syncytial embryo. Furthermore, the dRYBP protein physically interacts with SCE and PHO proteins. Finally, we also show that the C-terminal domain of dRYBP protein is required to produce the homeotic-like phenotypes. Our results suggest that *dRYBP* participates in the control of cell identity and in the control of cell proliferation and cell differentiation through a direct or an indirect interaction with PcG and trxG proteins.

MATERIALS AND METHODS

Drosophila strains and general procedures: The following mutations were employed: Pc^{3}, Sce^{1}, pho^{1}, pho^{cv}, trx^{E2}, Trl^{R85}, Trl^{13c}, $Rpd3^{1}$, and *Df (1)* ^{w67c23} flies (y^{-}, w^{-}) (all described in FlyBase, http://flybase.bio.indiana.edu/stocks). The *Df(2R) 58B3-59* (kindly provided by T. L. Orr-Weaver) deletes *dRYBP* and additional genes, and the PC-EGFP transgenic line (kindly provided by R. Paro) reproduces the expression of the Polycomb protein (Dietzel *et al.* 1999). The recombinant stock *dRYBP*^{1}, *P[Histone-3:GFP]/CyO* was made using flies containing *P[Histone-3:GFP]* on the second chromosome (provided by S. Aldaz). Genetic interactions between *dRYBP* and PcG/trxG mutations were studied, using stocks containing *P[SUPor-P]CG12190 [KG08683]* (Bellen *et al.* 2004) (herein called *dRYBP*^{1}) in the second chromosome and one of the PcG/trxG mutations on the third or the fourth chromosome. The number of flies examined ranged from 60 to 104. Homeotic transformations observed in these interaction studies appear to be very sensitive to crowding conditions, and therefore care was taken to avoid such conditions. Somatic heat-shocked induced clones were generated by crossing female *yw*^{1118} *P[hsp70-FLP122]; FRTG13, P[Ubi-GFPnls]2R2* with male *FRTG13, dRYBP*^{1}*/CyO* and by crossing female *yw*^{1118} *P[hsp70-FLP122] f*^{36a} *; FRT42D sha*^{1} *[forked*$^{+}$*]/CyO* with male *w*^{1118}*; FRT42D dRYBP*^{1}*/CyO*. The larval progenies of the different crosses were subjected to a 1-hr, 37° heat pulse at 24–48 hr or 48–72 hr or 72–96 hr after egg deposition. For overexpression experiments the GAL4/UAS system was used (Brand *et al.* 1994) at 25° and 29° with the lines *engrailed-GAL4* (*en-GAL4*) (Brand and Perrimon 1993), *cubitus-GAL4* (*ci-GAL4*), *armadillo-GAL4* (*arm-GAl4*) (Sanson *et al.* 1996), *Ultrabithorax-GAL4* (*Ubx-GAL4*) (Calleja *et al.* 1996), *scalloped-GAL4* (*sd-GAL4*) (Calleja *et al.* 1996), *daughterless-GAL4* (*da-GAL4*) (Wodarz *et al.* 1995), and *tubulin-GAL4* (*tub-GAL4*). To analyze the ovaries of the females, the virgins were crossed with males

and, after 3 days, the ovaries were dissected and stained with DAPI.

The lethal phase of the homozygous *dRYBP*^{I} was determined using a *dRYBP*^{I}*/CyOGFP* stock. Male and female *dRYBP*^{I}*/CyOGFP* were crossed and eggs (0–6 hr old) were collected, counted (~400 each experiment), and allowed to develop on plates [controls, using the *Df (1)*^{w67c23} flies, were done in parallel]. The "non-GFP" embryos were counted and their survival was monitored throughout development.

The fertility of the homozygous *dRYBP*^{I} females was determined by making crosses of a single homozygous *dRYBP*^{I} female with two *Df (1)*^{w67c23} males [controls were performed by crossing a single *Df (1)*^{w67c23} female with two *Df (1)*^{w67c23} males]. Similarly, the fertility of the homozygous *dRYBP*^{I} males was determined by making crosses of a single homozygous *dRYBP*^{I} male with two *Df (1)*^{w67c23} virgins [controls were made with a single *Df (1)*^{w67c23} male crossed to two *Df (1)*^{w67c23} females].

To study the effect of the *dRYBP* mutations on the syncytial nuclear divisions, we made a recombinant stock *dRYBP*^{I}*, P[Histone-3:GFP]/CyO.* We have previously confirmed that *P[Histone-3:GFP]/ P[Histone-3:GFP]* embryos do not show an aberrant nuclear division pattern. Female and male *dRYBP*^{I}*, P[Histone-3:GFP]/CyO* were crossed, embryos (0–3 hr old) were collected and fixed, and the pattern of nuclear divisions was observed. The syncytial mitotic phenotypes were variable in expressivity and penetrance. Also, the percentage of embryos showing mitotic phenotype was highly variable between experiments, making quantification very difficult. In this cross, the *dRYBP*^{I}*, P[Histone-3:GFP]* homozygous embryos were indistinguishable from the heterozygous embryos. Therefore to be sure that the mitotic phenotype was strictly maternal, we studied the pattern of nuclear divisions in embryos from female *dRYBP*^{I}*, P[Histone-3:GFP]/CyO* crossed with *Df (1)*^{w67c23} males. The syncytial mitotic phenotypes observed in the embryos from this cross were also variable in expressivity and penetrance. Finally, the potential influence of the balancer chromosome on the syncytial mitotic phenotype was excluded by studying the pattern of DAPI staining in the 3-hr-old embryos from females and males *P[Histone-3:GFP]/CyO.* For this, embryos were collected, fixed, and incubated with DAPI (5 μM in PBS) for 20 min; washed three times in PBS; and mounted for microscopic inspection. The pattern of nuclear divisions in these embryos was normal.

Studies of the lethality and of the cuticle embryonic phenotypes resulting from inactivation of *dRYBP* were performed using RNA interference. Males and females from the stocks *en-GAL4<UAS-dRYBP*$_{RNAi}$ or *ci-GAL4<UAS dRYBP*$_{RNAi}$ were allowed to lay eggs for 6 hr, and eggs were counted (~400 in each experiment) and allowed to develop on plates. Embryos were collected and mounted for microscopy analysis of the cuticle phenotypes, using standard methods.

Transgenic flies were obtained by standard procedures using *Df(1)*^{w67c23} (y^{-}, w^{-}) as host flies. The mounting of larvae and adult flies was performed using standard protocols. Wing size was measured by mounting the wings and next analyzing mounted wings, using the ImageJ image analysis software. With this software, the length of the margin of each mounted wing is determined and used to calculate the wing area. The mean area of multiple mounted wings was used for comparisons.

***P*-element mutagenesis and screening:** The stock *y*^{1}*w*^{1118}*; P{SUPor-P}CG12190 [KG08683]/CyO* (Bellen *et al.* 2004) that contains the markers *white*$^{+}$ and *yellow*$^{+}$ was used. Before starting the mutagenesis experiments, the stock was systematically outcrossed to clean possible second-site mutations. *y*^{1}*w*^{1118}*; P [y*$^{+}$ *w*$^{+}$ *KG08683]/CyO* were crossed with female *w*^{1118}*; Sp/CyO; Δ2-3 Dr/TM6Ubx.* Male progeny *w*^{1118}*; P [y*$^{+}$ *w*$^{+}$ *KG08683]/ CyO; Δ2-3 Dr/+* was individually crossed with female *y*^{1}*w*^{1118}*; Sco/ CyOwglacZ* and the *white*$^{-}$ progeny were scored to establish a stock. Genomic DNA was isolated and PCR was performed using the primers 5′-AACACTGGCTGCGCGTACTATCG-3′, 5′-GCG GGAGAGAAGACAACGACTCC-3′, and 5′-GTTCCACTAGCAG CGCCCATCCC-3′. PCR fragments were sequenced after analysis of fragment length. The precise excisions were checked for the lethality phenotype.

Immunohistochemistry: The antibody staining of embryos and imaginal discs was performed using standard protocols. The primary antibodies used were rabbit anti-DRYBP (1:100) (Bejarano *et al.* 2005), mouse anti-Ubx (1:10) (White and Wilcox 1984), mouse anti-Abd-B (1:20) (Celniker *et al.* 1990), rabbit anti-Abd-A (1:20) (Macias *et al.* 1990), rat anti-Antp (1:1500) (Reuter and Scott 1990), rabbit anti-Scr (1:100) (Glicksman and Brower 1988), mouse anti-en (1:200) (Patel *et al.* 1989), rat anti-ci (1:50) (Motzny and Holmgren 1995), rabbit anti-Pc (Wang *et al.* 2004), rabbit anti-Pho (1:10) (Brown *et al.* 1998), rabbit anti-Sce (1:200) (Gorfinkiel *et al.* 2004), mouse anti-cyclin A (Hibridoma Bank) (Knoblich and Lehner 1993), rabbit anti-GFP (1:300) (Invitrogen, San Diego), rabbit anti-activated caspase 3 (Cell Signaling Technologies), anti-BrdU (1:10) (Roche, Indianapolis), rabbit anti-β-gal (Cappel), mouse anti-β-gal (Promega, Madison, WI), rat anti-α-tubulin (1:500) (Seralab), mouse anti-Histone-H3 trimethyl Lys 27 (1:500) (Active Motif), and mouse anti-Psc (1:50) (Hybridoma Bank). To-Pro (Kiernan J 2001) and DAPI (Kiernan J 2001) were used to stain the DNA. Daunomycine (Chaires 1983) was used to label the nucleoli. Apoptosis was analyzed by Tunnel (*In Situ* Cell Death Detection kit TMR, Roche), acridine orange (Abrams *et al.* 1993), and anti-activated caspase 3 antibody stainings.

Expression constructs: The dRYBP-ΔCt and dRYBP-ΔZF fragments were generated by PCR amplification from the *dRYBP* cDNA (LD18758, Drosophila FlyBase). For dRYBP-ΔCt, the primers 5′-CATGTGCGACGTGCGGAAAGGAGGGATA CAAGGCCTC-3′ and 5′-GAGGCCTTGTATCCCTCCTTTCC GCACGTCGCACATG-3′ were used; for dRYBP-ΔZF the 5′-CCTCCTCTCCTCCTGTATTATGCCCAACGGGAAGTCC-3′ and 5′-GGACTTCCCGTTGGGCATAATACAGGAGGAGAG GAGG-3′ were used. The PCR fragments were cloned in pGEM and sequenced. The expression construct fragments were cloned in the pUAST vector and transgenic flies *P[UAS-dRYBP-ΔCt]* and *P[UAS-dRYBP-ΔZF]* were generated. The pUAST-dRYBP$_{RNAi}$ construct was made with a PCR-amplified 480-bp fragment obtained using 5′-CCCGGTACCGGGC TTTAAACGTGG-3′ and 5′-CCCGGATCCAGGAACCTCCAC GC-3′. The PCR product was cloned in pGEM-easy (Promega), generating pGEM-dRYBP-480$_{RNAi}$, which, after several cloning steps (details upon request) using the vector pHIBS (Nagel *et al.* 2002) and the vector pUAST, yielded pUAST-dRYBP$_{RNAi}$. This construct was injected to generate the *P[UAS-dRYBP*$_{RNAi}$*]* transgenic flies.

Quantitative PCR: RNA from first instar larvae and adult flies of the *Df(1)*^{w67c23}*, dRYBP*^{I}*/dRYBP*^{I}*, dRYBP* $^{\Delta 16}$*/dRYBP* $^{\Delta 16}$, and *Df(2R) 58B3-59/CyOGFP* genotypes was isolated by lysis and homogenization in TriZOL (Invitrogen), using a Pellet Motor (short pulses during 30 sec), followed by centrifugation (3 min, 13,000 rpm), chloroform/isopropanol extraction, ethanol precipitation, and resuspension in DEPC-water. Both the RT and the PCR reactions were done following the instructions accompanying the TaqMan predesigned gene-expression assay kit (Applied Biosystems, Foster City, CA) for Drosophila CG12190 (reference no.137861.2). RP49RNA (Foley *et al.* 1993) and 18srRNA primers and probes were used as controls.

Co-immunoprecipitaion, pull-down assays: *arm-GAL4>UAS-dRYBP* embryos were pelleted and lysed in 250 μl of lysis buffer containing 1% Triton X-100, 10 mM Tris (pH 7.4), 150 mM NaCl, 1 mM EDTA, 1mM EGTA pH 8, and protease inhibitors

(Complete Mini, Roche) at 4° for 15 min. After removing the cellular debris by centrifugation, 400 μg total protein lysate were incubated overnight with 25 μl 10 mg/ml BSA and 4 μg anti-SCE antibody or 6 μg of anti-β-gal antibody as a negative control. This mixture was then incubated with 30 μl of Protein-A Sepharose beads (Sigma-Aldrich) in PBS for 2 hr while rotating at 4°. The beads were collected and washed with lysis buffer four times at 4°. Proteins were eluted from the beads by heating with 20 μl of 2× PAGE loading buffer [200 mM DTT, 4% SDS, 100 mM Tris (pH 6.8), 20% glycerol, 0.1% bromophenol blue] at 100° for 5 min. The eluted fractions were resolved on a 15% PAGE gel system and transferred to a nitrocellulose membrane. After blocking, the membrane was incubated with anti-DRYBP antibody (1:500) followed by the appropriate secondary antibodies conjugated with horseradish peroxidase (HRP). Signals were detected with ECL reagents (Amersham, Arlington Heights, IL). We also attempted immunoprecipitation (IP) experiments with anti-PHO antibody. However, these experiments were not successful and, as a result, we performed pull-down assays to study the interaction with PHO.

Pull-down experiments used crude Drosophila extracts prepared by homogenizing 0.2 ml of third instar larvae in 0.4 ml of lysis buffer [1% NP-40, 1 mM PMSF, and protease inhibitor cocktail (Roche) in PBS]. The homogenates were centrifuged, and the aqueous supernatant was mixed with the full-length His-DRYBP protein [extracted under native conditions and purified by following the QIA express (QIAGEN, Valencia, CA) protocols]. The complexes were purified using Ni-NTA Agarose (QIAGEN) and washed five times in 0.5 M NaCl in PBS and one time in 50 mM Tris (pH 6.8). Proteins were eluted by boiling in loading buffer and resolved by 15% SDS–PAGE. After blotting to nitrocellulose, the membrane was incubated with anti-PHO antibody (1:500) and the signal was detected using the Amersham ECL Western blotting analysis system.

5′-RACE analysis: Total RNA was extracted from $Df(1)^{w67c23}$ (control) and from $dRYBP^{\Delta 55}/dRYBP^{\Delta 55}$ embryos as described above for quantitative PCR. cDNAs containing the 5′ transcript ends were identified using the 5′-RLM–RACE reagents (FirstChoice RLM–RACE kit; Ambion, Austin, TX), using the 5′ primer adaptor provided and the primer 5′-TTCCCGTT GGGCATGTTGACACTGGC-3′ based on the *dRYBP* sequence. The products were analyzed by agarose gel, isolated from the gel, cloned in pBluescript, and sequenced.

RESULTS

The *dRYBP* gene and dRYBP protein expression: The *dRYBP* gene (CG12190, FlyBase) is cytogenetically located at 58F7 and extends over 2.4 kb of genomic DNA (Figure 1A). 5′-RACE analysis shows that the transcription unit produces a single mRNA (Figure 1C). This transcript encodes a 150-aa protein (18 kDa) with a conserved amino terminus that includes an *N*pl4 zinc *f*inger (NZF) type zinc finger (Meyer *et al.* 2000, 2002) (Figure 1B). The carboxy terminus is conserved within the dRYBP proteins, but shows no similarity with any domains in the databases (Bejarano *et al.* 2005). Recently, a subgroup of the NZF domains (Wang *et al.* 2003; Alam *et al.* 2004) that include RYBP (Arrigoni *et al.* 2006) has been shown to possess ubiquitin-binding activity.

We have shown previously that the dRYBP protein is found in the oocyte nucleus, suggesting a maternal component of the protein (Bejarano *et al.* 2005). Moreover, its nuclear expression is observed ubiquitously and throughout development. A closer inspection of dRYBP distribution within the nucleus (Figure 2, A–H) reveals that it does not colocalize to either the heterochromatin (labeled with DAPI, Figure 2D) or the nucleoli (labeled with Daunomycine, Figure 2H). However, like the PcG proteins (Buchenau *et al.* 1998; Saurin *et al.* 1998; Netter *et al.* 2001; Ficz *et al.* 2005; Grimaud *et al.* 2006a), dRYBP is distributed in the nucleus in a discrete punctate pattern (Figure 2, A and E). We refer to these sites of protein localization as dRYBP nuclear bodies. Typically, there are of the order of ~30 small discrete spots plus one more prominent spot per nucleus (Figure 2A). The dRYBP nuclear bodies are similar to both PC nuclear bodies (Buchenau *et al.* 1998; Ficz *et al.* 2005; Grimaud *et al.* 2006a), which appear as small discrete spots, and Posterior sex combs nuclear bodies (Buchenau *et al.* 1998), which appear as a combination of small spots plus one prominent spot. We have studied whether dRYBP nuclear distribution colocalizes with PC [using the transgenic flies PC-EFGP (Dietzel *et al.* 1999)]. Additionally, we have studied whether dRYBP nuclear distribution colocalizes with the nuclear distribution of Histone H3 trimethyl Lys27 (H3K27me3) because it has been shown that H3K27me3 marks the PC nuclear bodies (T. Cheutin, personal communication). The results shown in Figure 2 indicate that some, but not all, of the dRYBP nuclear bodies colocalize with the PC bodies (Figure 2, A–C) and with the H3K27me3 nuclear bodies (Figure 2, E–G). The pattern of dRYBP distribution during the mitotic progression in the syncytial cell cycles of Drosophila embryos has been also analyzed. The first 13 mitotic divisions are synchronous and very rapid due to very abbreviated G_1 and G_2 phases and the absence of cytokinesis (Orr-Weaver 1994; Tram *et al.* 2001). Figure 2 shows the dynamic dRYBP distribution pattern throughout mitosis. dRYBP is dissociated from chromatin in prophase, remains visibly dissociated in metaphase (Figure 2, I–L), becomes associated with chromatin in anaphase (Figure 2, M–P), and remains bound in telophase. A similar dynamic pattern of distribution has also been observed for the Drosophila PC, PH, and PSC proteins (Buchenau *et al.* 1998).

Genetic and molecular characterization of *dRYBP* mutations: The *P*-element *P[KG08683]* or $P\{SUPor\text{-}P\}CG12190^{KG08683}$ (Bellen *et al.* 2004) is inserted in the 5′-UTR of the *dRYBP* gene (Figure 1A). This insertion, as described below, creates a null mutation in the *dRYBP* gene and we have therefore named it $dRYBP^{1}$. We have obtained two imprecise excisions from $dRYBP^{1}$: $dRYBP^{\Delta 16}$ and $dRYBP^{\Delta 55}$ (Figure 1A).

$dRYBP^{1}$ is classified as a null mutation because homozygous $dRYBP^{1}$ embryos and homozygous $dRYBP^{1}$

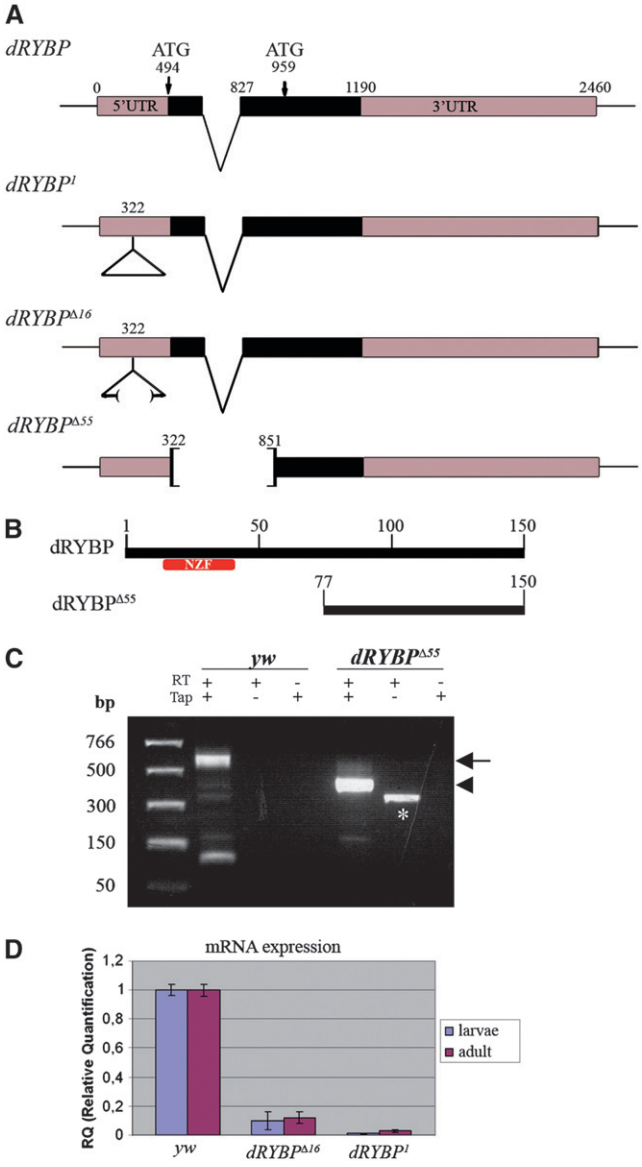

FIGURE 1.—Mutations in the *dRYBP* gene, 5′-RACE and quantitative PCR analysis. (A) The *dRYBP* gene structure, showing the positions of the two in-frame ATGs codons. *dRYBP*^{l} contains the *P[KG08683]*-element insertion (indicated as a triangle) at nucleotide position 322. *dRYBP*$^{\Delta 16}$ is an incomplete deletion of the *P[KG08683]* element. *dRYBP*$^{\Delta 55}$ deletes nucleotides 322–853. (B) The dRYBP protein contains an NZF domain (red) located in the amino terminus. The putative dRYBP$^{\Delta 55}$ protein encoded by *dRYBP*$^{\Delta 55}$ does not contain the NZF domain (red). (C) 5′-RACE analysis was performed using total RNA isolated from homozygous *Df(1)*^{w67c23} (*yw*) and homozygous *dRYBP*$^{\Delta 55}$ embryos. The reverse-transcription (RT) reaction was performed in the presence and in the absence of Tobacco acid pyrophosphatase (Tap). A control containing "minus-Tap"-treated RNA was also performed. A band of 560 bp (arrow) was observed, corresponding to the *dRYBP* wt 5′-RACE product (lane *yw*, "plus-RT/plus-Tap"; the smaller band in this lane is an artifact). A band of 380 bp (arrowhead) corresponds to the *dRYBP*$^{\Delta 55}$ 5′-RACE product (lane *dRYBP*$^{\Delta 55}$, plus-RT/plus-Tap). The band in the second lane of *dRYBP*$^{\Delta 55}$ (marked with *) corresponds to "plus-RT/minus-Tap" is an artifact of the 5′-RACE protocol used (Instructions manual, FirstChoice-RLM-RACE; Ambion). (D) Quantitative PCR results showing the relative mRNA expression levels from homozygous *Df(1)*^{w67c23} (*yw*), *dRYBP*^{l}, and *dRYBP*$^{\Delta 16}$ early first-instar larvae and adults.

adult flies do not express *dRYBP* mRNA (Figure 1D). However, dRYBP protein is seen in *dRYBP*^{l}/*dRYBP*^{l} embryos. We interpret this to be a result of the maternal contribution (see MATERIALS AND METHODS), as no protein is seen in the imaginal discs of *dRYBP*^{l}/*dRYBP*^{l} larvae.

All the phenotypes observed in embryos, larvae, and adults of the *dRYBP*^{l}/*dRYBP*^{l} genotypes are highly variable both in their penetrance and in their expressivity, and similar results were obtained when the phenotypes were studied in *dRYBP*^{l}/*Df(2R) 58B3–59*. Flies *dRYBP*^{l}/*dRYBP*^{l}are sublethal and show progressive lethality throughout development. Only 13% of the *dRYBP*^{l} homozygous embryos reached the adult stage, with 43% dying during embryogenesis and 44% during larval/pupal development. Moreover, *dRYBP*^{l}/*dRYBP*^{l} larvae show a significant developmental delay: it takes 10 days at 25° for *dRYBP*^{l}/*dRYBP*^{l} first-instar larvae to reach the pupal stage, instead of the normal 4–5 days (ASHBURNER 1989). Nearly all (90%) homozygous *dRYBP*^{l} females are sterile and, in most cases, oogenesis is arrested at stage 8 (ASHBURNER 1989) (Figure 3J). Finally, *dRYBP*^{l}/*dRYBP*^{l} adult flies from the few *dRYBP*^{l}/*dRYBP*^{l} fertile mothers crossed with *dRYBP*^{l}/*dRYBP*^{l} fathers present the same phenotypes described below for the homozygous *dRYBP*^{l} offspring from *dRYBP*^{l}/+ parents.

The homozygous embryos from *dRYBP*^{l}/+ parents that reach the stage of larval cuticle formation (~40%) show no detectable morphological cuticle defects. However, some embryos from *dRYBP*^{l}/+ parents (see MATERIALS AND METHODS) that die before cuticle formation (~60%) show severe defects in their pattern of nuclear division (Figure 3, compare A–D with E–H) and during mitotic progression. The nuclear divisions are asynchronic and large irregularly formed nuclei are often observed, most likely representing nuclei that did not divide (Figure 3, E–H).

Neither *dRYBP*^{l}/+ nor *dRYBP*^{l}/*dRYBP*^{l} flies show phenotypic similarities to flies with mutations in the PcG/trxG genes (SATO and DENELL 1985, 1987; BUSTURIA and MORATA 1988; BREEN and HARTE 1991). However, *dRYBP*^{l}/*dRYBP*^{l} flies do show other very weak and low-penetrance morphological defects, including the presence of a distal gap in vein L5 (21% of the flies, Figure 4B), malformed legs (11% of the flies, most frequently the mesothoracic leg), umbrella-shaped wings (54% of the flies), and two to three bristles on the sixth sternite in the males (5% of the flies). Finally, the size of the wings of the *dRYBP*^{l}/*dRYBP*^{l} flies is reduced 27% when compared with wild type (Figure 4E).

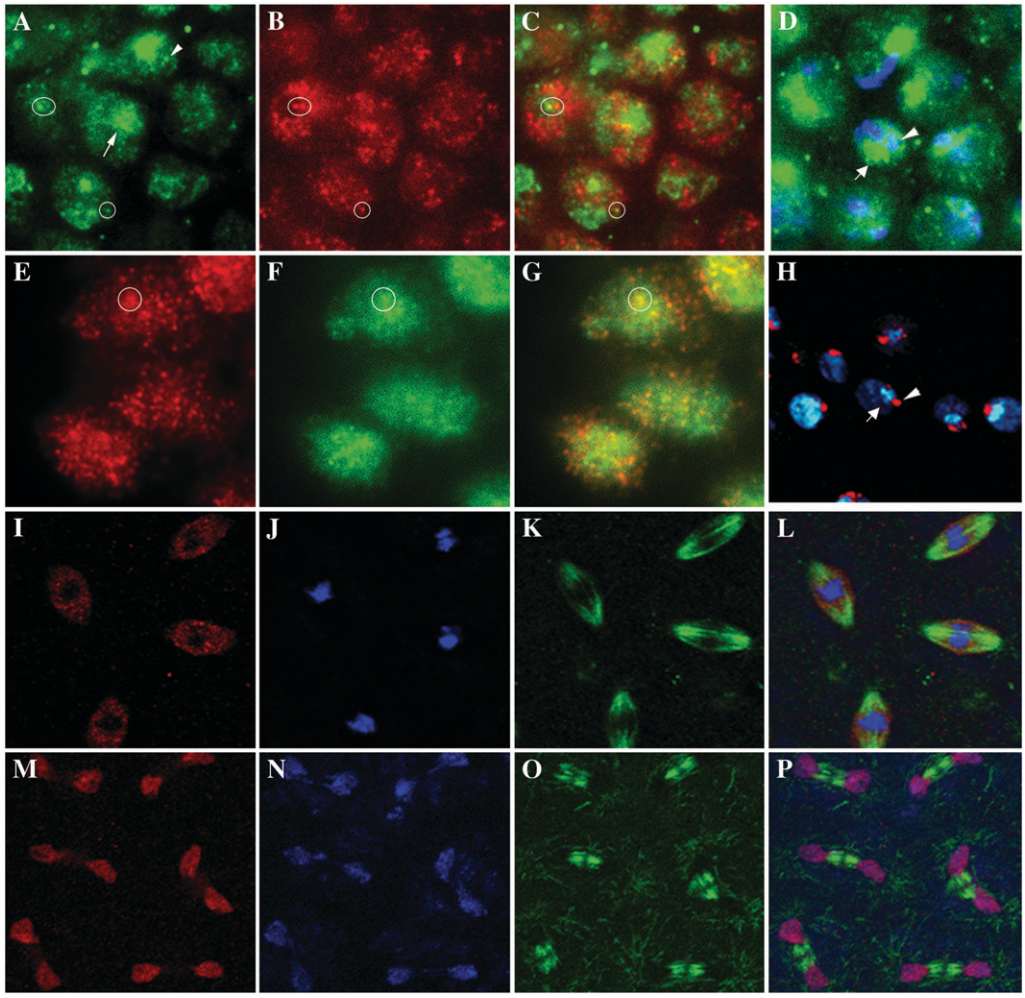

Figure 2.—Nuclear localization pattern of dRYBP protein. (A) dRYBP protein localization (green) in the embryonic nuclei. dRYBP nuclear bodies appear as both large (arrows) and small (arrowheads) structures. (B) H3K27me3 (red) colocalizes (circle) with dRYBP in some of the nuclear bodies (circle). (C) Merged image of A and B. The circles indicate colocalization in some of the bodies. (D) Staining of DAPI (blue) and dRYBP (green). (E) Embryonic nuclear distribution of dRYBP (red). (F) GFP nuclear localization of PC-EGFP transgenic embryos (circle indicates colocalization). (G) Merged image of E and F. (H) Daunomycine staining [used to label the nucleoli (red, arrowhead)] and dRYBP protein expression (blue, arrow) do not colocalize in the nuclei of the wing imaginal disc cells. (I–L) Localization of dRYBP protein (I, red), To-PRO (J, blue), and α-tubulin (K, green) during metaphase of syncytial embryonic nuclear divisions. dRYBP does not localize with To-PRO (J). (L) Merged image of I–K. (M–P) Localization of dRYBP protein (M, red), To-PRO (N, blue), and α-tubulin (O, green) during anaphase of syncytial embryonic nuclear divisions. dRYBP (red) colocalizes with To-PRO (blue). (P) Merged image of M–O.

Even though we see no homeotic-like phenotypes in *dRYBP* mutant flies, given that the gene has been proposed to belong to the PcG, we have studied the expression of the homeotic proteins Ultrabithorax (UBX) (White and Wilcox 1984), Abdominal-A (ABD-A) (Macias *et al.* 1990), and Abdominal-B (ABD-B) (Celniker *et al.* 1990; De Lorenzi and Bienz 1990) in homozygous $dRYBP^{1}$ embryos and larval imaginal discs. Expression of all these proteins was indistinguishable from wild type (data not shown).

The $dRYBP^{\Delta 16}$ mutation is an imprecise excision of the original $dRYBP^{1}$ that deletes 9 kb of the *P[KG08683]* element, but leaves the coding sequence of the *dRYBP* gene intact. *dRYBP* mRNA levels in $dRYBP^{\Delta 16}/dRYBP^{\Delta 16}$ embryos and adults are severely reduced (Figure 1D), indicating that $dRYBP^{\Delta 16}$ is a strong hypomorphic. The phenotypes of homozygous $dRYBP^{\Delta 16}$ adult flies are highly variable in their penetrance and expressivity and extremely similar to the phenotype described above for $dRYBP^{1}$.

$dRYBP^{\Delta 55}$ is a complete deletion of the *P[KG08683]* element that also removes 508 bp of the *dRYBP* gene (nucleotides 323–831; Figure 1A), including sequences of the 5′-UTR as well as the amino-terminal sequences encoding the NZF of the dRYBP protein. $dRYBP^{\Delta 55}/dRYBP^{\Delta 55}$ flies die progressively throughout development, are developmentally delayed, and, very infrequently, show the distal gap in the L5 vein, the umbrella-shaped wing, or the malformed mesothoracic leg phenotypes observed in the $dRYBP^{1}/dRYBP^{1}$ flies. However, $dRYBP^{\Delta 55}/dRYBP^{\Delta 55}$ females are not sterile and the $dRYBP^{\Delta 55}$ homozygotes can be maintained as a stock. 5′-RACE analysis indicates that a shortened *dRYBP* mRNA is produced in $dRYBP^{\Delta 55}/dRYBP^{\Delta 55}$ embryos (Figure 1C). This suggests that a truncated version of the dRYBP protein, most probably using the second in-frame ATG (Figure 1A), is produced in these flies. Finally, the expression levels and the cellular localization pattern of the truncated dRYBP protein in $dRYBP^{\Delta 55}/dRYBP^{\Delta 55}$ embryos and imaginal discs are very similar to those of the full-length proteins in wild-type (wt) tissues (Figure 2).

The analysis of *dRYBP* mutant phenotypes indicates that the gene is required for progression through

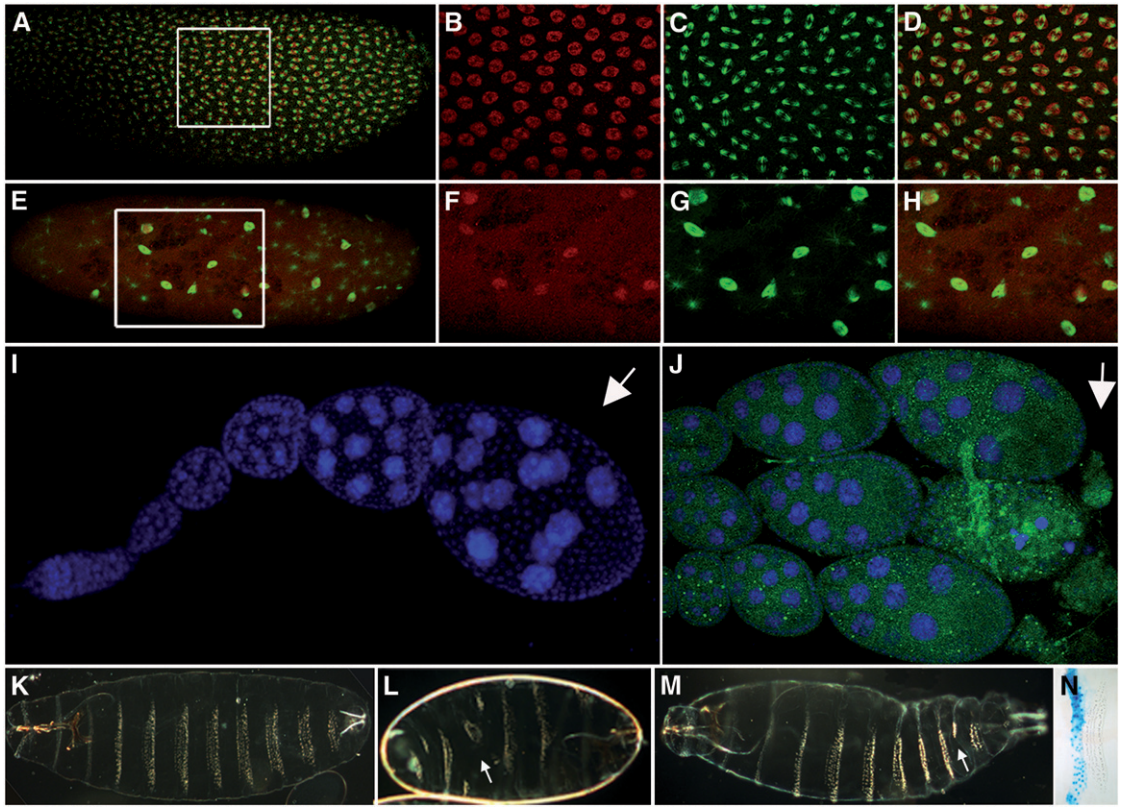

FIGURE 3.—*dRYBP* mutant phenotypes in the embryo. (A) Wild-type syncytial embryo stained with anti-dRYBP (red) and anti-α-tubulin (green) antibodies. There is a uniform distribution of nuclei along the embryo. (B–D) High magnification of the indicated area: dRYBP (B, red), α-tubulin (C, green), and merged (D). (E) Syncytial embryo from $dRYBP^{l}$/+ parents showing a mitotic collapse and the distribution of dRYBP protein (red) and α-tubulin (green). There are few nuclei and these are evenly distributed along the embryo. (F–H) High magnification of the indicated area: dRYBP (F, red), α-tubulin (G, green), and merged (H). (I) Wild-type ovariole stained with DAPI (blue) showing the stages of oogenesis (the arrow indicates stage 8 of oogenesis). (J) Ovariole from a homozygous $dRYBP^{l}$ female (the arrow indicates the degenerated stage 8 of oogenesis). (K) Wild-type first-instar larval cuticle showing the pattern of denticle belts (anterior to the left). (L) Example of an *en-Gal4>UAS-dRYBP-*$_{RNAi}$ embryo showing a severely disrupted pattern of the denticle belts along the entire embryonic cuticle (arrow indicates region lacking denticles). (M) Example of an *en-Gal4>UAS-dRYBP-*$_{RNAi}$ embryo showing a weak effect on the pattern of the denticle belts along the embryonic cuticle (arrow indicates the effect on the seventh abdominal segment). (N) β-Gal expression (blue) in an *en-Gal4>UAS-lacZ* larva showing the domain of expression of the *en-Gal4* line in the posterior compartment.

mitosis during the nuclear divisions of the syncytial embryos, perhaps accounting in part for the developmental delay that is also observed in *dRYBP* mutant larvae. Moreover, $dRYBP^{\Delta 55}/dRYBP^{\Delta 55}$ females are fertile, suggesting that the amino-terminal domain of the dRYBP protein is not required for its function in oogenesis.

Inactivation of *dRYBP* function by RNA interference: Phenotypes associated with the inactivation of the *dRYBP* function have been also studied by RNA interference (MONTGOMERY 2004), using UAS-*dRYBP-*$_{RNAi}$ constructs. The specificity of the inactivation was tested by examining the expression of dRYBP in *sd-GAL4>UAS-dRYBP>UAS-dRYBP-*$_{RNAi}$ imaginal discs. A strong reduction of dRYBP protein expression was observed (not shown). Moreover, the *sd-GAL4>UAS-dRYBP>UAS-dRYBP-*$_{RNAi}$ flies (not shown) showed rescue of the overexpression phenotypes seen in *sd-GAL4>UAS-dRYBP* (Figure 7D). The rescue might have resulted from a dilution of the *sd-GAL4* driver cause by the presence of two UAS-containing constructs (*UAS-dRYBP* and *UAS-dRYBP*$_{RNAi}$) instead of one (*UAS-dRYBP*). To control for this dilution possibility, we studied the dRYBP protein expression in imaginal discs and adult phenotypes of *sd-GAL4>UAS-dRYBP>UAS-GFP* (not shown).

The *ci-GAL4* and the *en-GAL4* lines drive expression throughout development in the anterior and the posterior compartments, respectively, and have been used to inactivate *dRYBP* function. *en-Gal4>UAS-dRYBP-*$_{RNAi}$ flies exhibit progressive lethality throughout embryonic and larval development (~50% of the embryos die during embryogenesis). The larval cuticle phenotypes of the *en-Gal4>UAS-dRYBP-*$_{RNAi}$ embryos that survive to secrete cuticle show an aberrant pattern of segmentation with severe disruption in the pattern of the denticle belts, but no detectable homeotic transformations (Figure 3, L and M). The phenotype is highly variable both in penetrance and in expressivity.

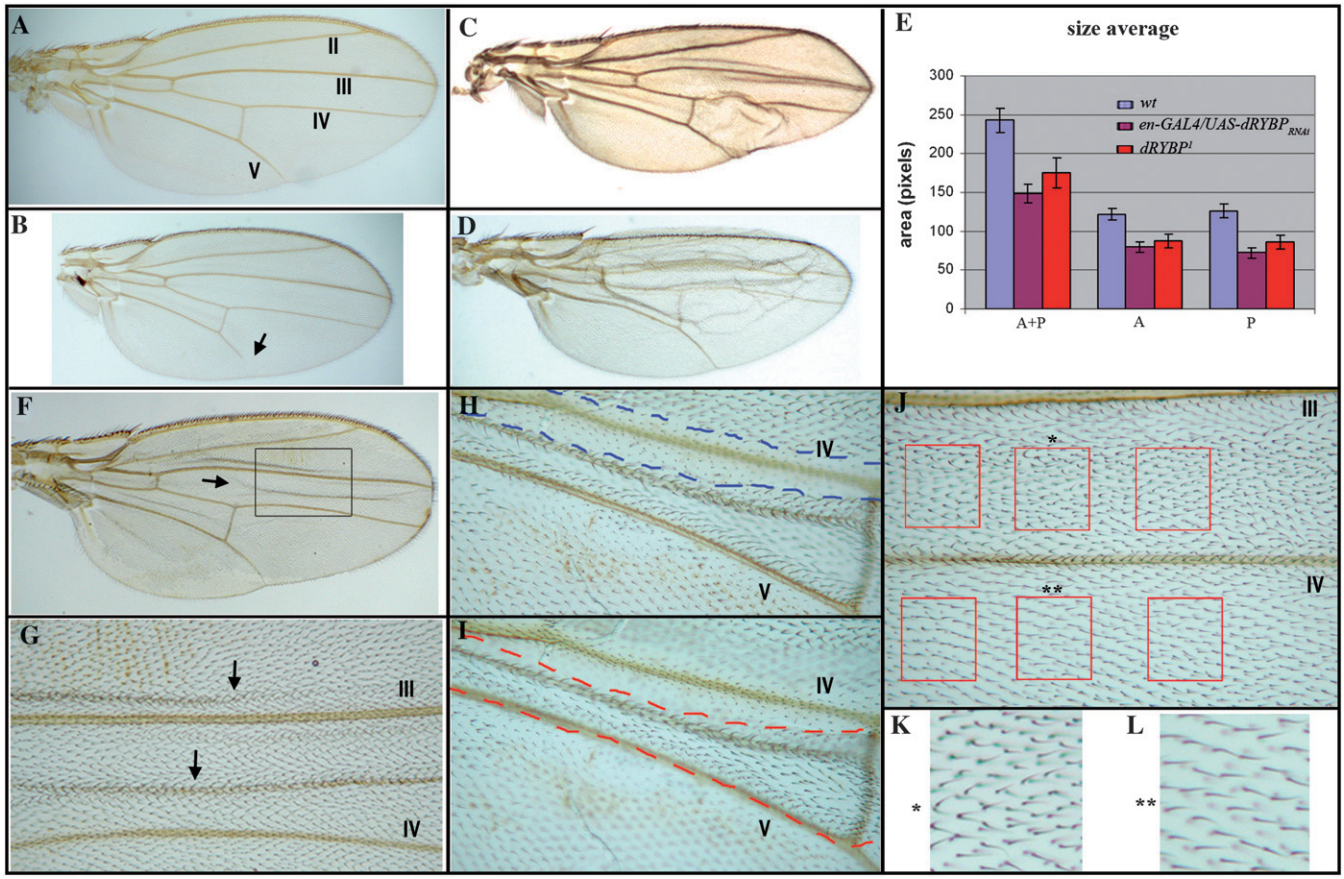

FIGURE 4.—*dRYBP* mutant phenotypes in the adult wings. (A) Wing from a wild-type male fly. The numbers of the veins are indicated. (B) Wing from a homozygous $dRYBP^{1}$ male showing a reduction of the wing size and a distal gap in vein V (arrow). (C) Wing from an *en-Gal4>UAS-dRYBP-*$_{RNAi}$ male showing the blister in the posterior compartment and a reduction in wing size. (D) Wing from a *ci-Gal4>UAS-dRYBP-*$_{RNAi}$ male showing the blister in the anterior compartment and a reduction in wing size. (E) Area of wild-type male wings (blue), *en-Gal4>UAS-dRYBP-*$_{RNAi}$ male wings (purple), and homozygous $dRYBP^{1}$ (red). "A+P" indicates entire wing area; "P" indicates area of the posterior compartment; "A" indicates area of the anterior compartment. (F) Wing containing somatic homozygous $dRYBP^{1}$ mutant clones marked with *forked* and twin clones marked with *shavenoid*. The presence of mutant clones results in the formation of blisters (one of them is indicated with an arrow). (G) High magnification of the area indicated in F showing two blisters (arrows). (H) Ventral view of the wing containing $dRYBP^{1}$ mutant clones marked with *forked* (dashed red line labels the *forked* clone) between veins IV and V, where the presence of the clone induces the appearance of a blister on the dorsal surface of the wing. (I) Dorsal view of the same wing (dashed blue line labels the *shavenoid* clone). (J) $dRYBP^{1}$ mutant clone marked with *forked* between veins III and IV. The red squares identify an example of the areas chosen to calculate the trichome density in the mutant clones (*forked*) *vs.* the density of trichomes in the corresponding wild-type areas (red squares at bottom). (K) High magnification of the mutant *forked* area (marked with *). (L) High magnification of the wild-type area (marked with **). The density of trichomes is higher in K than in L.

Interestingly, the inactivation of *dRYBP* in the cells of the posterior compartments in the *en-Gal4>UAS-dRYBP-*$_{RNAi}$ embryos appears to have a nonautonomous effect in the adjacent cells of the anterior compartment: the pattern of both the anterior and the posterior compartments is disrupted (Figure 3L).

The wings of surviving *en-Gal4>UAS-dRYBP-*$_{RNAi}$ (Figure 4C) and of *ci-Gal4>UAS-dRYBP-*$_{RNAi}$ (Figure 4D) flies are blistered in the posterior and anterior compartments, respectively. Curiously, the overall size of the wings is reduced (Figure 4, compare A with C and D). Although the blistered-wings phenotype complicates the size quantifications, when wing size in the *en-Gal4>UAS-dRYBP-*$_{RNAi}$ flies is measured, an overall reduction of 40% is observed compared to the wild type (Figure 4E), with a 43% reduction in the posterior compartment and a 35% reduction in the anterior compartment. This, once again, indicates a nonautonomous effect in the wild-type cells of the anterior compartment. The most likely explanation for this phenomenon is the "accommodation effect" first described by GARCIA-BELLIDO *et al.* (1994). Interestingly, the inactivation of the *dRYBP* function, by RNA interference, in the whole wing using the ubiquitous *arm-GaL4*, *da-Gal4*, and *tub-GaL4* drivers did not produce blistered wings (not shown), suggesting that the generation of the wing phenotypes observed in *en-Gal4>UAS-dRYBP-*$_{RNAi}$ and *ci-Gal4>UAS-dRYBP-*$_{RNAi}$ requires the contact of wild-type and mutant cells. Finally, the expression of the UBX protein in the wing and haltere imaginal

discs from *en-Gal4>UAS-dRYBP-$_{RNAi}$* and *ci-Gal4>UAS-dRYBP-$_{RNAi}$* larvae was normal (data not shown).

The disrupted-pattern phenotypes observed in embryos and the reduction of the wing size observed in the adults lacking *dRYBP* function prompted us to characterize the pattern of apoptosis in embryos and imaginal discs of the genotypes *dRYBP^{1}/dRYBP^{1}*, *en-Gal4>UAS-dRYBP-$_{RNAi}$*, and *ci-Gal4>UAS-dRYBP-$_{RNAi}$*. This was done by staining imaginal discs and embryos with acridine orange (Abrams *et al.* 1993) as well as analyzing the expression of both Tunnel and the activated form of caspase-3 (Lee and Luo 1999), each serving as markers of cell death. In all these assays, no differences in the pattern of apoptosis between *dRYBP* mutant and wild-type tissues were seen (data not shown).

The proliferation and aberrant mitosis phenotypes found in embryos from *dRYBP^{1}*/+ parents, as well as the reduced wing size in *en-Gal4>UAS-dRYBP-$_{RNAi}$* and *dRYBP^{1}/dRYBP^{1}*, could be caused by a disruption in cell-cycle progression. The Cdk1/cyclin A and Cdk1/cyclin B complexes control progression through mitosis (for a review see Deshpande *et al.* 2005). We therefore analyzed cyclin A (Knoblich and Lehner 1993) expression in *en-Gal4>UAS-dRYBP-$_{RNAi}$* wing imaginal discs. Cyclin A expression was identical in both the anterior and the posterior compartments of the wing disc (not shown).

Requirement of *dRYBP* throughout larval development: Somatic mutant clones of *dRYBP* were induced at different times during development, using the null allele *dRYBP^{1}* and the FLP/FRT system. We first induced homozygous *dRYBP^{1}* mutant clones in the wing disc, marked with GFP expression, to study the size of the mutant clones compared to the corresponding twin clones and to analyze the expression of the homeotic UBX and ABD-B proteins. The homozygous *dRYBP^{1}* mutant clones and the corresponding wild-type twin clones were of similar size (not shown) and no ectopic expression of either UBX or ABD-B proteins was seen (data not shown). To study the phenotype of the homozygous *dRYBP^{1}* mutant clones in the adult fly, we induced mutant clones marked with *forked* (*f*) (Lindsley and Zimm 1992) and wild-type twin clones marked with *shavenoid* (*sha*) (Lindsley and Zimm 1992). No homeotic transformations were found in the adult mutant clones. However, and independently of the time of clone induction, a number of observations were made: first, *forked* clones and *shavenoid* clones were of similar size, suggesting that the proliferation rates were not affected in the mutant clones; second, in ~30% of the clones studied, the presence of a *forked* clone on either one of the wing surfaces (ventral or dorsal) caused the appearance of a blister on the opposite surface (Figure 4, F–I). Finally, the *forked* mutant clones showed an increase in cell density. We calculated a 20% reduction in the number of wild-type trichomes compared to the *forked* clones (Figure 4, J–L). The phenotypes of these clones indicate that *dRYBP* is required for cellular differentiation throughout larval development. The developmental requirement of *dRYBP* was also studied, using the *UAS-dRYBP-$_{RNAi}$* constructs to repress dRYBP expression in the imaginal discs. The blistered-wing phenotype (similar to that shown in Figure 4, C and D) was observed regardless of the time of clone induction (at 24–48, 48–72, and 72–96 hr after egg laying).

***dRYBP* genetic and molecular interactions:** The observed absence of homeotic phenotypes associated with lack of *dRYBP* function is not consistent with the proposed classification of *dRYBP* as a member of the *PcG* genes. Therefore, we studied whether *dRYBP* mutations genetically interact with mutations in the *PcG* and *trxG* genes. To this end, we used the *dRYBP^{1}*, *Pc^{3}*, *Sce^{1}*, *pho^{1}*, *pho^{cv}*, *Trl^{R85}*, *trx^{E2}*, and *Rpd3^{1}* mutant alleles and scored for either enhancement or suppression of the *dRYBP*- and the *PcG/trxG*-associated phenotypes. Adult flies *dRYBP^{1}/dRYBP^{1}; Pc^{3}*/+, *dRYBP^{1}/dRYBP^{1}; Trl^{R85}*/+, *dRYBP^{1}/dRYBP^{1}; Rpd3^{1}*/+, *dRYBP^{1}/dRYBP^{1}; pho^{1}*/+, and *dRYBP^{1}/dRYBP^{1}; pho^{1}/pho^{cv}* showed no enhancement or suppression of homeotic phenotypes. Furthermore, embryos and imaginal discs from *dRYBP^{1}/CyO; Pc^{3}*/+, *dRYBP^{1}/CyO; Rpd3^{1}*/+, and *dRYBP^{1}/CyO; Trl^{R85}*/+ showed no altered expression of the UBX or ABD-B proteins (data not shown).

In contrast, *dRYBP^{1}/dRYBP^{1}; Sce^{1}*/+ males showed an increased number of sex combs in the meso- and metathoracic legs when compared with *Sce^{1}*/+ males or with siblings *dRYBP^{1}*/+; *Sce^{1}*/+. Surprisingly, *dRYBP^{1}/dRYBP^{1}; Sce^{1}*/+ males showed depigmentation of the fifth abdominal segment (Figure 5, B and E), a phenotype never seen in either *Sce^{1}*/+ or *dRYBP^{1}*/+; *Sce^{1}*/+ males. Additionally, *dRYBP^{1}/dRYBP^{1}; trx^{E2}*/+ males (Figure 5D) showed an increased percentage of individuals exhibiting depigmentation of the fifth abdominal segment when compared with sibling *dRYBP^{1}*/+; *trx^{E2}*/+ males or *trx^{E2}*/+ males (Figure 5C). The expressivity of the depigmentation phenotype was strongly increased compared to the depigmentation of the abdomen of *trx^{E2}*/+ males. No differences in ABD-B protein expression pattern were seen between *dRYBP^{1}/dRYBP^{1}; Sce^{1}/Sce^{1}* and *Sce^{1}/Sce^{1}* embryos. Likewise no differences in ABD-B protein expression pattern were observed between *dRYBP^{1}/dRYBP^{1}; trx^{E2}/trx^{E2}* and *trx^{E2}/trx^{E2}* embryos (not shown).

Possible molecular interactions between dRYBP and SCE and PHO were studied using immunoprecipitation and pull-down experiments. The dRYBP protein was found to interact with SCE and PHO proteins (Figure 5, F and G). The results of both the genetic and the molecular-interaction experiments indicate that the dRYBP protein interacts genetically with both PcG and the trxG proteins and molecularly with the PcG proteins SCE and PHO.

Function of the dRYBP protein domains in the generation of homeotic–like phenotypes: Overexpression of the dRYBP protein has been shown to generate homeotic-like phenotypes that can be modulated by

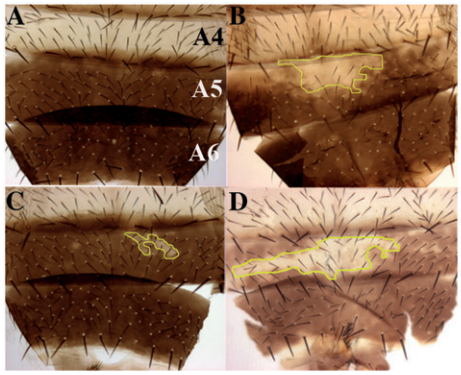

E

	Sex-comb in T2 and T3 legs (%)	De-pigmentation in A5 (%)
+/+; +/+	0	0
Sce^{1}/+	0	0
$dRYBP^{1}/dRYBP^{1}$;Sce^{1}/+	42	68
$dRYBP^{1}$/+; trx^{E2}/+	ND	52
$dRYBP^{1}/dRYBP^{1}$; trx^{E2}/+	ND	95

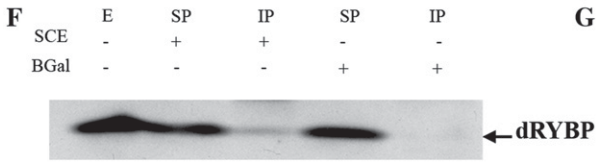

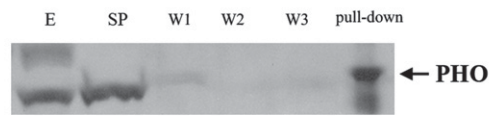

FIGURE 5.—*dRYBP* genetic and molecular interactions. (A) Dorsal abdomen of a wild-type adult male showing the A4, A5, and A6 segments. The A5 and A6 segments are pigmented. (B) Dorsal abdomen of a $dRYBP^{1}/dRYBP^{1}$; Sce^{1}/+ male showing patches of depigmentation of the A5 segment. (C) Dorsal abdomen of a trx^{E2}/+ male showing patches of depigmentation of the A5 segment. (D) Dorsal abdomen of an $dRYBP^{1}/dRYBP^{1}$; trx^{E2}/+ male showing patches of depigmentation. (E) Percentage of flies showing the extra sex comb phenotype in T2 and T3 legs and the depigmentation phenotype in the A5 segment of the males. ND: not determined. (F) dRYBP protein co-immunoprecipitates with SCE but not with BGAL used as a control. Shown is a Western blot of the IP with SCE antibody and BGAL antibody revealed with anti-dRYBP antibody. E, extract; SP, supernatant; IP, immunoprecipitation. (G) dRYBP protein pulls down the PHO protein. Shown is a Western blot of the dRYBP pull down revealed with anti-PHO antibody. E, extract; SP, supernatant; W, washes.

mutations in the PcG/trxG genes (BEJARANO *et al.* 2005). Interestingly, and depending on the cellular context, high levels of dRYBP caused either the ectopic expression or the repression of the homeotic UBX protein (BEJARANO *et al.* 2005 and Figure 7, C and I). To further investigate the role *dRYBP* plays in the regulation of homeotic genes, we analyzed the effects of overexpression of dRYBP in different cellular contexts and studied the function of the domains of the dRYBP protein in the generation of the homeotic-like phenotypes. We used the *arm-GAL4* line, which drives the expression ubiquitously and throughout development (SANSON *et al.* 1996), the *Ubx-Gal4* line, which drives the expression in the haltere and third leg imaginal disc (DE NAVAS *et al.* 2006), and the *sd-GAL4* line, which drives the expression in the wing and haltere imaginal discs.

Ubx-Gal4>UAS-dRYBP flies exhibit ectopic sex combs on the metathoracic (third) legs (Figure 6, B–E). Sex comb identity is determined by the *Sex comb reduced* (*Scr*) gene (STRUHL 1982; PATTATUCCI and KAUFMAN 1991), and the homeotic Sex comb reduced (SCR) protein is expressed in the prothoracic (first) leg imaginal disc (Figure 6F), but not in the second (mesothoracic) or third leg discs. We looked at the expression of SCR (GLICKSMAN and BROWER 1988) in *Ubx-Gal4>UAS-dRYBP* imaginal leg discs and found that it is ectopically expressed in the third imaginal leg discs (Figure 6, G–I). It is important to note that SCR expression only partially overlaps with the domain where dRYBP is overexpressed (Figure 6, G–I). The *arm-Gal4>UAS-dRYBP* flies also occasionally showed ectopic sex combs in the second and third legs (not shown). Moreover, *arm-Gal4>UAS-dRYBP* males showed the Miscadestral pigmentation (Mcp) (LEWIS 1978) and the Ultra-abdominal (Uab) (LEWIS 1978) phenotypes. The Mcp phenotype consists of ectopic pigmentation in the fourth abdominal segment (Figure 6, K and M) and the Uab phenotype consists of the appearance, in the first abdominal segment, of long bristles morphologically characteristic of posterior abdominal segments (Figure 6, K and L). Although these phenotypes result from the misexpression of the homeotic proteins (LEWIS 1978; BUSTURIA *et al.* 1989; CELNIKER *et al.* 1990; MACIAS *et al.* 1990; SANCHEZ-HERRERO 1991), we could find no misregulation of ABD-A and ABD-B homeotic proteins in *arm-Gal4>UAS-dRYBP* embryos.

A functional analysis of dRYBP protein domains was performed by expressing the *UAS-dRYBP-ΔZF* and *UAS-dRYBP-ΔCt* constructs. *dRYBP-ΔZF* deletes the protein's amino-terminal domain that contains the NZF sequences (amino acids 1–70, MATERIALS AND METHODS, Figure 7A); *dRYBP-ΔCt* deletes the protein's carboxy-terminal domain (amino acids 70–150).

*sd-Gal4>UAS-dRYBP-*ΔCt flies showed no wing or haltere phenotypes. We looked at the expression of dRYBP protein in the wing imaginal discs and observed a weak and diffused expression (not shown), suggesting either that the dRYBP-ΔCt protein is not stable or that it is not fully recognized by the anti-dRYBP antibody.

sd-Gal4>UAS-dRYBP-ΔZF flies exhibit transformation of wings toward haltere, as indicated by the appearance

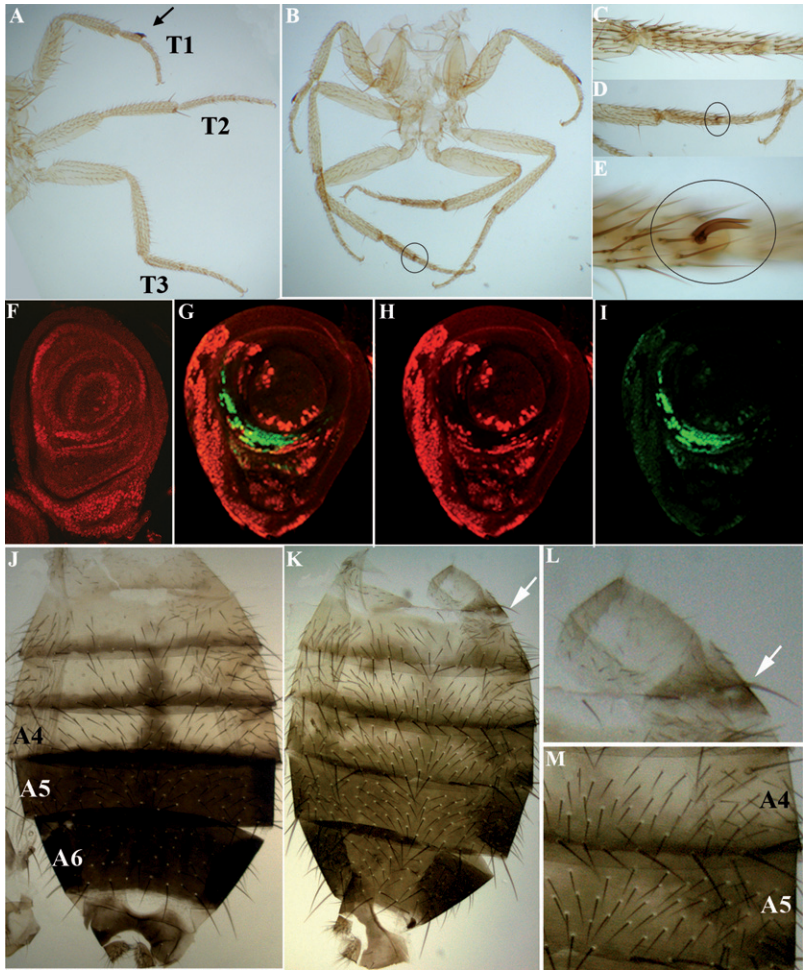

FIGURE 6.—Overexpression of dRYBP in the leg and abdomen. (A) Legs (T1, T2, and T3) of a wild-type male. The T1 leg shows the sex comb in the basitarso (arrow). (B) Legs from an *Ubx-Gal4>UAS-dRYBP* male showing the appearance of an extra sex comb on the T3 leg (circle). (C) Basitarso of a wild-type male T3 leg. (D–E) Higher magnification of the basitarso shown in B (circles). (F) Expression of the SCR protein (red) in a wt male T1 leg imaginal disc. (G) Merged expression of dRYBP (red) and SCR (green) in the *Ubx-Gal4>UAS-dRYBP* T3 leg imaginal disc. The expression of SCR does not completely overlap with the expression of dRYBP. (H) Expression of dRYBP (red). (I) Expression of SCR (green). (J) Abdomen of a wild-type male showing the A4, A5, and A6 segments. A5 and A6 are pigmented. (K) Abdomen of an *arm-Gal4>UAS-dRYBP* male showing the Uab phenotype (long bristles in the A1 segment marked by an arrow) and the Mcp phenotype (ectopic pigmentation in the A4 segment). (L) Higher magnification of Uab phenotype shown in K. (M) Higher magnification of Mcp phenotype shown in K.

of haltere-like trichomes in the wing (Figure 7H). This transformation is likely mediated by the ectopic expression of UBX in the wing disc (Figure 7, C and F). The phenotype in the wings and the ectopic expression of UBX in the *sd-Gal4>UAS-dRYBP-ΔZF* wing imaginal discs were very similar to those of *sd-Gal4>UAS-dRYBP* (Figure 7, D and G, and BEJARANO *et al.* 2005). Moreover, in both cases the ectopic expression of UBX did not completely overlap with the domain of dRYBP overexpression. Curiously, we observed that the dRYBP protein in the imaginal discs of *sd-Gal4>UAS-dRYBP-ΔZF* larvae is, primarily, localized outside the nucleus, suggesting that this truncated protein might be functional outside the nucleus.

A haltere phenotype consisting of small-size haltere covered with wing-like trichomes was seen in both *sd-Gal4>UAS-dRYBP-ΔZF* and *Ubx-Gal4>UAS-dRYBP-ΔZF* flies (Figure 7, M and R). The haltere discs of both *sd-Gal4>UAS-dRYBP-ΔZF* and *Ubx-Gal4>UAS-dRYBP-ΔZF* (Figure 7, N–P) larvae showed repression of the UBX expression, as was seen with the overexpression of *UAS-dRYBP* (Figure 7, I–K).

These results indicate that the carboxy terminus is required while the amino terminus is dispensable for the repression of UBX in the haltere disc and for the ectopic expression of UBX in the wing discs, both mediated by the overexpression of the dRYBP protein.

DISCUSSION

The *dRYBP* loss-of-function phenotypes are remarkable in the high variability of both their penetrance and their expressivity. Given the current knowledge of *dRYBP* function, it is difficult to explain the dramatic phenotypic variability. A striking illustration of this is that some embryos experience complete mitotic collapse (Figure 3, E–H) while others (Figure 4B) develop completely to adulthood. As there are no genes in the Drosophila genome that are clearly homologous to *dRYBP*, it is unlikely that this is due to the existence of homologous proteins that replace *dRYBP* function at a given developmental time.

It is possible that *dRYBP* phenotypic variability reflects on the robustness of the embryos, which is dependent on the fitness of the mother as well as the extrinsic and intrinsic environmental perturbations to which the flies are exposed (STELLING *et al.* 2004; FRIEDMAN and PERRIMON 2007). *dRYBP* function might remain "latent" in the cell until the requirement becomes essential in response, for example, to specific stress

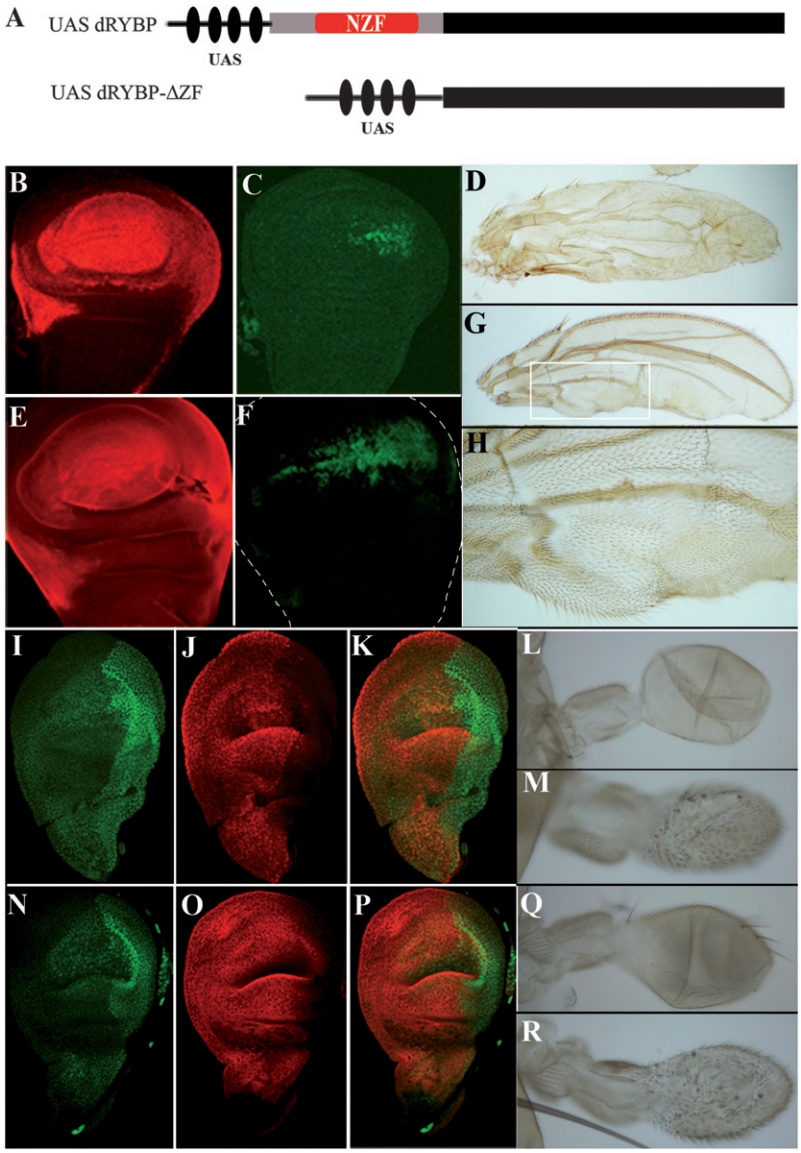

FIGURE 7.—Overexpression of dRYBP in the wing and haltere imaginal discs: function of the carboxy-terminal domain. (A) Scheme of the UAS-dRYBP and UAS-dRYBP-ΔZF (lacking the NFZ domain) constructs. (B) Expression of dRYBP (red) in a *sd-Gal4>UAS-dRYBP* wing imaginal disc. (C) Expression of UBX (green) in a *sd-Gal4>UAS-dRYBP* wing imaginal disc. (D) Wing of a *sd-Gal4>UAS-dRYBP* fly. (E) Expression of dRYBP (red) in a *sd-Gal4>UAS-dRYBP-ΔZF* wing imaginal disc. (F) Expression of UBX (green) in a *sd-Gal4>UAS-dRYBP-ΔZF* wing imaginal disc. (G) Wing of a *sd-Gal4>UAS-dRYBP-ΔZF* fly showing the trichomes typical of the haltere. (H) Higher magnification of the indicated area in G to show the haltere-like trichomes. (I–K) Expression of UBX (I, green) and DRYBP (J, red) in an *Ubx-Gal4>UAS-dRYBP* haltere disc (K, merged). (L) Wild-type haltere. (M) *Ubx-Gal4>UAS-dRYBP* haltere, showing the trichomes similar to the wing trichomes. (Q) *Ubx-Gal4* haltere. The *Ubx-Gal4* line is inserted in the *Ubx* gene and shows the haploinsufficient *Ubx* phenotype consisting of the appearance of some hairs in the capitelum (compare with L). (N–P) Expression of UBX (N, green) and dRYBP (O, red) in an *Ubx-Gal4>UAS-dRYBP-ΔZF* haltere disc (P, merged). (R) Haltere of an *Ubx-Gal4>UAS-dRYBP-ΔZF* fly.

conditions. Stress of this type could happen during the rapid nuclear divisions that take place in the syncytial embryo or when, in addition to the removal of the dRYBP protein, an intrinsic perturbation is introduced, *i.e.*, modifying the genetic background by introducing mutations in other genes. In both cases, depending on the robustness of the individual, cells lacking *dRYBP* function may respond either by terminating mitosis (Figure 3, E–H) or by affecting morphological development (Figure 5, A–E).

Another characteristic of *dRYBP* inactivation are the differences between the phenotypes caused by null mutations and those caused by RNA interference. For example, $dRYBP^{1}/dRYBP^{1}$ embryos that reach the stage of cuticle formation do not show larval cuticle morphological defects. In contrast, *en-Gal4>UAS-dRYBP-*$_{RNAi}$ larvae show severe cuticle defects (Figure 3, L and M). Additionally, the wings of $dRYBP^{1}/dRYBP^{1}$ flies do not show the blistered phenotype observed in *en-Gal4>UAS-dRYBP-*$_{RNAi}$ or *ci-Gal4>UAS-dRYBP-*$_{RNAi}$ flies (Figure 4, C and D). A trivial explanation for these phenotypic differences is that the *UAS-dRYBP-*$_{RNAi}$ construct, in addition to inactivating the expression of *dRYBP*, is also inactivating the function of other genes. We have seen reduced dRYBP expression and rescue of the overexpression phenotypes in *sd-Gal4>UAS-dRYBP, UAS-dRYBP-*$_{RNAi}$ imaginal discs and adults, suggesting that *dRYBP* inactivation using *UAS-dRYBP-*$_{RNAi}$ is quite specific. A more attractive and plausible explanation is that the phenotypes caused by inactivation of *dRYBP* function are strongly revealed when wild-type cells are in physical contact with *dRYBP* mutant cells. This idea is supported by several observations. First, $dRYBP^{1}/dRYBP^{1}$ mutant clones in the wing, where wild-type and *dRYBP* mutant cells are in contact, cause a blistered phenotype (Figure 4, F–L) similar to that seen in *en-Gal4>UAS-dRYBP-*$_{RNAi}$ and *ci-Gal4>UAS-dRYBP-*$_{RNAi}$ (Figure 4, C and D). Second, $dRYBP^{1}/dRYBP^{1}$ larvae do not show

cuticle defects while *en-Gal4>UAS-dRYBP-$_{RNAi}$*, in which mutant cells physically contact wild-type cells, show strong and nonautonomous phenotypes (Figure 3, L and M). Third, wings of *da-Gal4>UAS-dRYBP-$_{RNAi}$*, *tub-Gal4>UAS-dRYBP-$_{RNAi}$*, and *arm-Gal4>UAS-dRYBP-$_{RNAi}$* flies, in which mutant cells are not in contact with wild-type cells because *da-Gal4*, *tub-Gal4*, and *arm-Gal4* inactivate dRYBP in all the wing cells, did not show the blistered phenotype. The study of the factors involved in the generation of these nonautonomous defects will facilitate the understanding of dRYBP function in the process of cellular differentiation.

dRYBP involvement in the mechanisms of PcG/trxG—expression of the protein, genetic analysis, and molecular interactions: dRYBP expression is restricted to the nonnucleoli portion of the nucleus and forms a pattern of discrete spots very similar to the so-called PcG nuclear bodies reported for the PC, PH, and PSC proteins. Like PSC, the dRYBP nuclear expression pattern consists of both large and small bodies, numbering ~30 per embryonic nucleus (Buchenau *et al.* 1998; Saurin *et al.* 1998; Dietzel *et al.* 1999; Netter *et al.* 2001; Ficz *et al.* 2005; Grimaud *et al.* 2006a) (Figure 2A). The partial overlap of dRYBP and PC distribution in the nuclear bodies (Figure 2, C and G) suggests that dRYBP functions, together with PcG, in the regulation of a subset of PcG target genes. Moreover, it also indicates that dRYBP, independently of PcG, is involved in the regulation of other processes.

dRYBP (Figure 2, I–P) and PcG proteins show similar dynamic mitotic distribution patterns during the nuclear cycles in the syncytial embryo (Abrams *et al.* 1993; Buchenau *et al.* 1998; Netter *et al.* 2001; Martinez *et al.* 2006; O'Dor *et al.* 2006). This distribution pattern may indicate a role for the protein in the regulation of cell-cycle progression because *dRYBP* mutant syncytial embryos exhibit a severe disruption in the pattern of nuclear divisions (Figure 3, E–H). The involvement of PcG/trxG proteins in the regulation of cell-cycle progression has been proposed. For example, Polycomb response elements (PREs) have been identified in the cell-cycle regulator *cyclin A* gene (Martinez *et al.* 2006) while mutations in *ph*, *Pc*, and *Psc*, all members of the PcG, show severe defects in chromosomal segregation (O'Dor *et al.* 2006). The dRYBP protein might very well participate with PcG/trxG in this process.

A role for *dRYBP* in mitotic progression and control of cell proliferation may explain the slow larval growth observed in *dRYBP^{1}/dRYBP^{1}* and the reduction of the wing size when *dRYBP* is inactivated (Figure 4, B–D). Furthermore, the described increase in cell density observed in *dRYBP* mutant clones (Figure 4, F–L) suggests that the gene might also have a role in cell differentiation.

The interactions described between loss-of-function *dRYBP* mutations and mutations in *Sce* (a PcG) and the *trx* (a trxG) genes show that *dRYBP* participates in the maintenance of both the repressed transcriptional states controlled by the PcG genes and the active transcriptional states controlled by the trxG genes. The interaction with mutations of the *Sce* gene exhibits enhancement of the Pc-like phenotype (*i.e.*, increased number of sex combs) and enhancement of the trx-like phenotype (*i.e.*, increased depigmentation of the fifth abdominal segment). We have observed a molecular interaction between PHO and dRYBP proteins (Figure 5G). However, we did not find a genetic interaction between mutations in both genes, using the *dRYBP^{1}* and the *pho^{1}* and *pho^{cv}* mutant alleles. The *dRYBP^{1}/dRYBP^{1}; pho^{1}/+* flies do not show homeotic phenotypes and the *dRYBP^{1}/dRYBP^{1}; pho^{1}/pho^{cv}* flies do not show enhancement or suppression of the number of ectopic sex combs observed in *pho^{1}/pho^{cv}* flies. We believe that this is probably due to the strong maternal effect of the PHO protein (Breen and Duncan 1986). We have shown that the dRYBP and SCE proteins physically interact. It has been shown that the murine RYBP protein is a novel ubiquitin-binding protein that is itself ubiquitinated (Arrigoni *et al.* 2006). Furthermore, it has been shown that the RING1B, the mouse SCE homolog and a known ubiquitin E3 ligase, promotes RYBP ubiquitination (Arrigoni *et al.* 2006). The observed interaction between *dRYBP* and *Sce* suggests that this may be the case in Drosophila as well. The interaction with mutations in the *trx* gene clearly shows that *dRYBP* is able to interact not only with PcG complexes, but also with trxG.

dRYBP involvement in the mechanisms of PcG/trxG—analysis of the overexpression phenotypes: High levels of the dRYBP protein generate homeotic-like phenotypes in the legs, wings, haltere, and abdomen of flies (Figures 6 and 7). The carboxy-terminal domain of the dRYBP protein is sufficient to cause misexpression of the homeotic proteins to generate the homeotic-like phenotypes (Figures 6 and 7). For example, the appearance of extra sex combs in the metathoracic legs results from the ectopic expression of the homeotic Sex comb-reduced protein (Figure 6), while the transformation of wing into haltere (Figure 7, D–H) results from the ectopic expression of the UBX protein (Figure 7C).

Curiously, overexpression of dRYBP in the wing and leg imaginal discs does not result in the ectopic expression of UBX and SCR throughout the entire overexpression domain (Figure 6). This suggests that there is a partial inactivation of the PcG proteins in these regions, which could be due to transcriptional repression of PcG genes or to sequestration of PcG proteins. We investigated whether PC expression is decreased in *en-GAL4>UAS-dRYBP* wing imaginal discs and found no difference between the anterior and the posterior compartments (not shown). This indicates that the homeotic-like phenotypes are probably due to sequestration of the PcG proteins mediated by dRYBP overexpression. This possibility is supported by the observed

modulation of the homeotic phenotypes by PcG and trxG mutations (Bejarano *et al.* 2005). The proposed sequestration of the PcG/trxG protein complexes is mediated through the carboxy terminus of the protein, as the ectopic expression of the UBX protein in the wing disc results from the overexpression of both the full-length dRYBP and the dRYBP-ΔZF proteins (Figure 7).

The phenotypes associated with the overexpression of some PcG/trxG proteins have been reported (Martin and Adler 1993; Peterson *et al.* 2004). Psc and Su(z)2 have been overexpressed by heat treatment of the transgenic flies containing hs-Psc and hs-Su(z)2 and neither one shows mutant phenotypes in any tissue (Martin and Adler 1993). Overexpression of the SPM domain of the Sex comb in midleg (SCM) protein produces homeotic-like phenotypes that can be modulated by PcG mutations (Peterson *et al.* 2004). Perhaps genes of PcG/trxG involved in recruitment or aggregation of PcG/trxG proteins produce, when overexpressed, sequestration of PcG/trxG proteins and, therefore, homeotic-like phenotypes.

Within the haltere, where homeotic-like phenotypes are also produced by the carboxy-terminal domain of the dRYBP protein, the effect of high-level dRYBP expression on UBX expression is distinct: UBX expression is repressed throughout the entire domain of dRYBP overexpression. As a result, the adult haltere shows a phenotypic transformation toward wing but without taking on the size and shape of a wing (Figure 7, M and R). Recently, it has been shown that the size of the haltere is determined by the combined levels of decapentaplegic (DPP) and UBX (de Navas *et al.* 2006). Perhaps high levels of dRYBP expression repress Dpp expression and this, together with the reduction of UBX expression, results in the small-haltere phenotype (Figure 7, M and R). Further characterization of this phenomenon may allow the separation of the mechanisms of size regulation and differentiation.

Here we have presented an examination of the phenotypes associated with inactivation of the *dRYBP* gene and an initial functional and biochemical characterization of the dRYBP protein. *dRYBP* was previously classified as a PcG gene on the basis of the protein molecular interactions and the phenotypes resulting from its overexpression (Garcia *et al.* 1999; Bejarano *et al.* 2005). However, the results from the present study indicate that *dRYBP* is a PcG- and trxG-interacting gene that participates in many biological processes, but it is not a "classical" PcG gene because *dRYBP* loss-of-function mutations do not show homeotic phenotypes. This demonstrates the danger of classification of a gene function based on overexpression phenotypes. Our results indicate that *dRYBP* is a PcG- and trxG-interacting gene that participates, together with PcG/trxG, in the mechanisms of cell-identity control. Furthermore, these results should provide the basis for a more complete description and understanding of the mechanisms in which *dRYBP* is involved, including the control of the nuclear divisions in the syncytial embryo and the regulation of cell differentiation.

We are very grateful to Fernando Diaz Benjumea, Keith Harshman, and Ernesto Sánchez-Herrero for discussions and critically reading the manuscript. We especially thank Fernando Diaz Benjumea for his help with the somatic *dRYBP* mutant clones and Thierry Cheutin and people of the laboratory of Giacomo Cavalli for their help with the dRYBP/PC/H3K27m3 colocalization experiments; Miguel A. Vidal for discussions; Judy Kassis, Richard Jones, and Isabel Guerrero for the PHO, PC, and SCE antibodies, respectively; Terry Orr-Weaver, Renato Paro, and the Bloomington Stock Center for fly stocks; Rocio Simón for help with some of the experiments; and the Madrid Drosophila community for reagents and discussions. This work was supported by grants from Dirección General de Investigación Científica y Técnica (BMC-2002-00524 and BFU-2005-02319) and the Fundación Investigación Médica Mutua Madrileña (FMM-2006) to A.B. and by an institutional grant to the Centro de Biología Molecular Consejo Superior de Investigaciones Cientificas–Universidad Autónoma de Madrid from Fundación Ramón Areces.

LITERATURE CITED

Abrams, J. M., K. White, L. I. Fessler and H. Steller, 1993 Programmed cell death during Drosophila embryogenesis. Development **117:** 29–43.

Alam, S. L., J. Sun, M. Payne, B. D. Welch, B. K. Blake *et al.*, 2004 Ubiquitin interactions of NZF zinc fingers. EMBO J. **23:** 1411–1421.

Arrigoni, R., S. L. Alam, J. A. Wamstad, V. J. Bardwell, W. I. Sundquist *et al.*, 2006 The Polycomb-associated protein Rybp is a ubiquitin binding protein. FEBS Lett. **580:** 6233–6241.

Ashburner, M., 1989 *Drosophila: A Laboratory Handbook*. Cold Spring Harbor Laboratory Press, Cold Spring Harbor, NY.

Bejarano, F., I. González, M. Vidal and A. Busturia, 2005 The *Drosophila RYBP* gene functions as a *Polycomb*-dependent transcriptional repressor. Mech. Dev. **122:** 1118–1129.

Bellen, H. J., R. W. Levis, G. Liao, Y. He, J. W. Carlson *et al.*, 2004 The BDGP gene disruption project: single transposon insertions associated with 40% of Drosophila genes. Genetics **167:** 761–781.

Brand, A. H., and N. Perrimon, 1993 Targeted gene expression as a means of altering cell fates and generating dominant phenotypes. Development **118:** 401–415.

Brand, A. H., A. S. Manoukian and N. Perrimon, 1994 Ectopic expression in Drosophila. Methods Cell Biol. **44:** 635–654.

Breen, T. R., and I. M. Duncan, 1986 Maternal expression of genes that regulate the bithorax complex of Drosophila melanogaster. Dev. Biol. **118:** 442–456.

Breen, T. R., and P. J. Harte, 1991 Molecular characterization of the trithorax gene, a positive regulator of homeotic gene expression in Drosophila. Mech. Dev. **35:** 113–127.

Brock, H. W., and C. L. Fisher, 2005 Maintenance of gene expression patterns. Dev. Dyn. **232:** 633–655.

Brown, J. L., D. Mucci, M. Whiteley, M. L. Dirksen and J. A. Kassis, 1998 The Drosophila Polycomb group gene pleiohomeotic encodes a DNA binding protein with homology to the transcription factor YY1. Mol. Cell **1:** 1057–1064.

Buchenau, P., J. Hodgson, H. Strutt and D. J. Arndt-Jovin, 1998 The distribution of polycomb-group proteins during cell division and development in Drosophila embryos: impact on models for silencing. J. Cell Biol. **141:** 469–481.

Busturia, A., and G. Morata, 1988 Ectopic expression of homeotic genes caused by the elimination of the Polycomb gene in Drosophila imaginal epidermis. Development **104:** 713–720.

Busturia, A., J. Casanova, E. Sanchez-Herrero, R. Gonzalez and G. Morata, 1989 Genetic structure of the abd-A gene of Drosophila. Development **107:** 575–583.

Calleja, M., E. Moreno, S. Pelaz and G. Morata, 1996 Visualization of gene expression in living adult Drosophila. Science **274:** 252–255.

Cao, R., L. Wang, H. Wang, L. Xia, H. Erdjument-Bromage *et al.*, 2002 Role of histone H3 lysine 27 methylation in Polycomb-group silencing. Science **298:** 1039–1043.

Cao, R., Y. Tsukada and Y. Zhang, 2005 Role of Bmi-1 and Ring1A in H2A ubiquitylation and Hox gene silencing. Mol. Cell **20:** 845–854.

Celniker, S. E., S. Sharma, D. J. Keelan and E. B. Lewis, 1990 The molecular genetics of the bithorax complex of Drosophila: cis-regulation in the Abdominal-B domain. EMBO J. **9:** 4277–4286.

Chaires, J. B., 1983 Daunomycin inhibits the B leads to Z transition in poly d(G-C). Nucleic Acids Res. **11:** 8485–8494.

Czermin, B., R. Melfi, D. McCabe, V. Seitz, A. Imhof *et al.*, 2002 Drosophila enhancer of Zeste/ESC complexes have a histone H3 methyltransferase activity that marks chromosomal Polycomb sites. Cell **111:** 185–196.

De Lorenzi, M., and M. Bienz, 1990 Expression of Abdominal-B homoeproteins in Drosophila embryos. Development **108:** 323–329.

de Napoles, M., J. E. Mermoud, R. Wakao, Y. A. Tang, M. Endoh *et al.*, 2004 Polycomb group proteins Ring1A/B link ubiquitylation of histone H2A to heritable gene silencing and X inactivation. Dev. Cell **7:** 663–676.

de Navas, L. F., D. L. Garaulet and E. Sanchez-Herrero, 2006 The ultrabithorax Hox gene of Drosophila controls haltere size by regulating the Dpp pathway. Development **133:** 4495–4506.

Deshpande, A., P. Sicinski and P. W. Hinds, 2005 Cyclins and cdks in development and cancer: a perspective. Oncogene **24:** 2909–2915.

Dietzel, S., H. Niemann, B. Bruckner, C. Maurange and R. Paro, 1999 The nuclear distribution of Polycomb during Drosophila melanogaster development shown with a GFP fusion protein. Chromosoma **108:** 83–94.

Fang, J., T. Chen, B. Chadwick, E. Li and Y. Zhang, 2004 Ring1b-mediated H2A ubiquitination associates with inactive X chromosomes and is involved in initiation of X inactivation. J. Biol. Chem. **279:** 52812–52815.

Ferres-Marco, D., I. Gutierrez-Garcia, D. M. Vallejo, J. Bolivar, F. J. Gutierrez-Avino *et al.*, 2006 Epigenetic silencers and Notch collaborate to promote malignant tumours by Rb silencing. Nature **439:** 430–436.

Ficz, G., R. Heintzmann and D. J. Arndt-Jovin, 2005 Polycomb group protein complexes exchange rapidly in living Drosophila. Development **132:** 3963–3976.

Foley, K. P., M. W. Leonard and J. D. Engel, 1993 Quantitation of RNA using the polymerase chain reaction. Trends Genet. **9:** 380–385.

Friedman, A., and N. Perrimon, 2007 Genetic screening for signal transduction in the era of network biology. Cell **128:** 225–231.

Garcia, E., C. Marcos-Gutierrez, M. del Mar Lorente, J. C. Moreno and M. Vidal, 1999 RYBP, a new repressor protein that interacts with components of the mammalian Polycomb complex, and with the transcription factor YY1. EMBO J. **18:** 3404–3418.

Garcia-Bellido, A., F. Cortes and M. Milan, 1994 Cell interactions in the control of size in Drosophila wings. Proc. Natl. Acad. Sci. USA **91:** 10222–10226.

Gatti, M., and B. S. Baker, 1989 Genes controlling essential cell-cycle functions in Drosophila melanogaster. Genes Dev. **3:** 438–453.

Gearhart, M. D., C. M. Corcoran, J. A. Wamstad and V. J. Bardwell, 2006 Polycomb group and SCF ubiquitin ligases are found in a novel BCOR complex that is recruited to BCL6 targets. Mol. Cell. Biol. **26:** 6880–6889.

Glicksman, M. A., and D. L. Brower, 1988 Expression of the Sex combs reduced protein in Drosophila larvae. Dev. Biol. **127:** 113–118.

Gorfinkiel, N., L. Fanti, T. Melgar, E. Garcia, S. Pimpinelli *et al.*, 2004 The Drosophila Polycomb group gene Sex combs extra encodes the ortholog of mammalian Ring1 proteins. Mech. Dev. **121:** 449–462.

Grimaud, C., F. Bantignies, M. Pal-Bhadra, P. Ghana, U. Bhadra *et al.*, 2006a RNAi components are required for nuclear clustering of Polycomb group response elements. Cell **124:** 957–971.

Grimaud, C., N. Negre and G. Cavalli, 2006b From genetics to epigenetics: the tale of Polycomb group and trithorax group genes. Chromosome Res. **14:** 363–375.

Jürgens, G., 1985 A group of genes controlling the spatial expression of the bithorax complex in *drosophila*. Nature **316:** 153–155.

Kiernan, J. A., 2001 Classification and naming of dyes, stains and fluorochromes. Biotech. Histochem. **76:** 261–279.

Klymenko, T., B. Papp, W. Fischle, T. Kocher, M. Schelder *et al.*, 2006 A Polycomb group protein complex with sequence-specific DNA-binding and selective methyl-lysine-binding activities. Genes Dev. **20:** 1110–1122.

Knoblich, J. A., and C. F. Lehner, 1993 Synergistic action of Drosophila cyclins A and B during the G2-M transition. EMBO J. **12:** 65–74.

Kodjabachian, L., M. Delaage, C. Maurel, R. Miassod, B. Jacq *et al.*, 1998 Mutations in ccf, a novel Drosophila gene encoding a chromosomal factor, affect progression through mitosis and interact with Pc-G mutations. EMBO J. **17:** 1063–1075.

Kuzmichev, A., K. Nishioka, H. Erdjument-Bromage, P. Tempst and D. Reinberg, 2002 Histone methyltransferase activity associated with a human multiprotein complex containing the Enhancer of Zeste protein. Genes Dev. **16:** 2893–2905.

Lee, T., and L. Luo, 1999 Mosaic analysis with a repressible cell marker for studies of gene function in neuronal morphogenesis. Neuron **22:** 451–461.

Lewis, E. B., 1978 A gene complex controlling segmentation in Drosophila. Nature **276:** 565–570.

Lindsley, D., and G. Zimm, 1992 *The Genome of Drosophila melanogaster.* Academic Press, New York.

Macias, A., J. Casanova and G. Morata, 1990 Expression and regulation of the abd-A gene of Drosophila. Development **110:** 1197–1207.

Martin, E. C., and P. N. Adler, 1993 The Polycomb group gene Posterior Sex Combs encodes a chromosomal protein. Development **117:** 641–655.

Martinez, A. M., and G. Cavalli, 2006 The role of polycomb group proteins in cell cycle regulation during development. Cell Cycle **5:** 1189–1197.

Martinez, A. M., S. Colomb, J. Dejardin, F. Bantignies and G. Cavalli, 2006 Polycomb group-dependent Cyclin A repression in Drosophila. Genes Dev. **20:** 501–513.

Meyer, H. H., J. G. Shorter, J. Seemann, D. Pappin and G. Warren, 2000 A complex of mammalian ufd1 and npl4 links the AAA-ATPase, p97, to ubiquitin and nuclear transport pathways. EMBO J. **19:** 2181–2192.

Meyer, H. H., Y. Wang and G. Warren, 2002 Direct binding of ubiquitin conjugates by the mammalian p97 adaptor complexes, p47 and Ufd1-Npl4. EMBO J. **21:** 5645–5652.

Montgomery, M. K., 2004 The use of double-stranded RNA to knock down specific gene activity. Methods Mol. Biol. **260:** 129–144.

Motzny, C. K., and R. Holmgren, 1995 The Drosophila cubitus interruptus protein and its role in the wingless and hedgehog signal transduction pathways. Mech. Dev. **52:** 137–150.

Muller, J., C. M. Hart, N. J. Francis, M. L. Vargas, A. Sengupta *et al.*, 2002 Histone methyltransferase activity of a Drosophila Polycomb group repressor complex. Cell **111:** 197–208.

Nagel, A. C., D. Maier and A. Preiss, 2002 Green fluorescent protein as a convenient and versatile marker for studies on functional genomics in Drosophila. Dev. Genes Evol. **212:** 93–98.

Netter, S., M. Faucheux and L. Theodore, 2001 Developmental dynamics of a polyhomeotic-EGFP fusion in vivo. DNA Cell Biol. **20:** 483–492.

O'Dor, E., S. A. Beck and H. W. Brock, 2006 Polycomb group mutants exhibit mitotic defects in syncytial cell cycles of Drosophila embryos. Dev. Biol. **290:** 312–322.

Orr-Weaver, T. L., 1994 Developmental modification of the Drosophila cell cycle. Trends Genet. **10:** 321–327.

Otte, A. P., and T. H. Kwaks, 2003 Gene repression by Polycomb group protein complexes: A distinct complex for every occasion? Curr. Opin. Genet. Dev. **13:** 448–454.

Patel, N. H., E. Martin-Blanco, K. G. Coleman, S. J. Poole, M. C. Ellis *et al.*, 1989 Expression of engrailed proteins in arthropods, annelids, and chordates. Cell **58:** 955–968.

Pattatucci, A. M., and T. C. Kaufman, 1991 The homeotic gene Sex combs reduced of *Drosophila melanogaster* is differentially regulated in the embryonic and imaginal stages of development. Genetics **129:** 443–461.

Peterson, A. J., D. R. Mallin, N. J. Francis, C. S. Ketel, J. Stamm *et al.*, 2004 Requirement for sex comb on midleg protein inter-

actions in Drosophila polycomb group repression. Genetics **167:** 1225–1239.

Phillips, M. D., and A. Shearn, 1990 Mutations in polycombeotic, a Drosophila polycomb-group gene, cause a wide range of maternal and zygotic phenotypes. Genetics **125:** 91–101.

Pirity, M. K., J. Locker and N. Schreiber-Agus, 2005 Rybp/DEDAF is required for early postimplantation and for central nervous system development. Mol. Cell. Biol. **25:** 7193–7202.

Reuter, R., and M. P. Scott, 1990 Expression and function of the homoeotic genes Antennapedia and Sex combs reduced in the embryonic midgut of Drosophila. Development **109:** 289–303.

Ringrose, L., and R. Paro, 2004 Epigenetic regulation of cellular memory by the Polycomb and Trithorax group proteins. Annu. Rev. Genet. **38:** 413–443.

Sanchez, C., I. Sanchez, J. A. Demmers, P. Rodriguez, J. Strouboulis *et al.*, 2007 Proteomics analysis of Ring1B/Rnf2 interactors identifies a novel complex with the Fbxl10/Jhdm1B histone demethylase and the Bcl6 interacting corepressor. Mol. Cell Proteomics **6:** 820–834.

Sanchez-Herrero, E., 1991 Control of the expression of the bithorax complex genes abdominal-A and abdominal-B by cis-regulatory regions in Drosophila embryos. Development **111:** 437–449.

Sanson, B., P. White and J. P. Vincent, 1996 Uncoupling cadherin-based adhesion from wingless signalling in Drosophila. Nature **383:** 627–630.

Sato, T., and R. E. Denell, 1985 Homoeosis in Drosophila: anterior and posterior transformations of Polycomb lethal embryos. Dev. Biol. **110:** 53–64.

Sato, T., and R. E. Denell, 1987 Homoeosis in Drosophila: the lethal syndrome of the regulator of bithorax (or trithorax) locus and its interaction with other homoeotic loci. Genetics **116:** 389–398.

Saurin, A. J., C. Shiels, J. Williamson, D. P. Satijn, A. P. Otte *et al.*, 1998 The human polycomb group complex associates with pericentromeric heterochromatin to form a novel nuclear domain. J. Cell Biol. **142:** 887–898.

Sawa, C., T. Yoshikawa, F. Matsuda-Suzuki, S. Delehouzee, M. Goto *et al.*, 2002 YEAF1/RYBP and YAF-2 are functionally distinct members of a cofactor family for the YY1 and E4TF1/hGABP transcription factors. J. Biol. Chem. **277:** 22484–22490.

Schlisio, S., T. Halperin, M. Vidal and J. R. Nevins, 2002 Interaction of YY1 with E2Fs, mediated by RYBP, provides a mechanism for specificity of E2F function. EMBO J. **21:** 5775–5786.

Schuettengruber, B., D. Chourrout, M. Vervoort, B. Leblanc and G. Cavalli, 2007 Genome regulation by polycomb and trithorax proteins. Cell **128:** 735–745.

Schwartz, Y. B., and V. Pirrotta, 2007 Polycomb silencing mechanisms and the management of genomic programmes. Nat. Rev. Genet. **8:** 9–22.

Shao, Z., F. Raible, R. Mollaaghababa, J. Guyon, C. Wu *et al.*, 1999 Stabilization of chromatin structure by PRC1, a Polycomb complex. Cell **9:** 37–46.

Sparmann, A., and M. van Lohuizen, 2006 Polycomb silencers control cell fate, development and cancer. Nat. Rev. Cancer **6:** 846–856.

Stelling, J., U. Sauer, Z. Szallasi, F. J. Doyle, 3rd and J. Doyle, 2004 Robustness of cellular functions. Cell **118:** 675–685.

Struhl, G., 1982 Genes controlling segmental specification in the Drosophila thorax. Proc. Natl. Acad. Sci. USA **79:** 7380–7384.

Tram, U., B. Riggs and W. Sullivan, 2001 *Cleavage and Gastrulation in Drosophila Embryos* (Encyclopedia of Life Sciences). Nature Publishing Group, London.

Trimarchi, J. M., B. Fairchild, J. Wen and J. A. Lees, 2001 The E2F6 transcription factor is a component of the mammalian Bmi1-containing polycomb complex. Proc. Natl. Acad. Sci. USA **98:** 1519–1524.

Valk-Lingbeek, M. E., S. W. Bruggeman and M. van Lohuizen, 2004 Stem cells and cancer; the polycomb connection. Cell **118:** 409–418.

van der Lugt, N. M., J. Domen, K. Linders, M. van Roon, E. Robanus-Maandag *et al.*, 1994 Posterior transformation, neurological abnormalities, and severe hematopoietic defects in mice with a targeted deletion of the bmi-1 proto-oncogene. Genes Dev. **8:** 757–769.

Wang, B., S. L. Alam, H. H. Meyer, M. Payne, T. L. Stemmler *et al.*, 2003 Structure and ubiquitin interactions of the conserved zinc finger domain of Npl4. J. Biol. Chem. **278:** 20225–20234.

Wang, H., L. Wang, H. Erdjument-Bromage, M. Vidal, P. Tempst *et al.*, 2004 Role of histone H2A ubiquitination in Polycomb silencing. Nature **431:** 873–878.

White, R. A., and M. Wilcox, 1984 Protein products of the bithorax complex in Drosophila. Cell **39:** 163–171.

Wodarz, A., U. Hinz, M. Engelbert and E. Knust, 1995 Expression of crumbs confers apical character on plasma membrane domains of ectodermal epithelia of Drosophila. Cell **82:** 67–76.

Communicating editor: K. G. Golic